AD-A124 723 MODAL CONTROL OF A SATELLITE IN AN UNSTABLE ORBIT ABOUT 1/1
L3(U) AIR FORCE INST OF TECH WRIGHT-PATTERSON AFB OH
SCHOOL OF ENGINEERING F M DEARMOND DEC 82
UNCLASSIFIED AFIT/GAE/AA/82D-7 F/G 22/3 NL

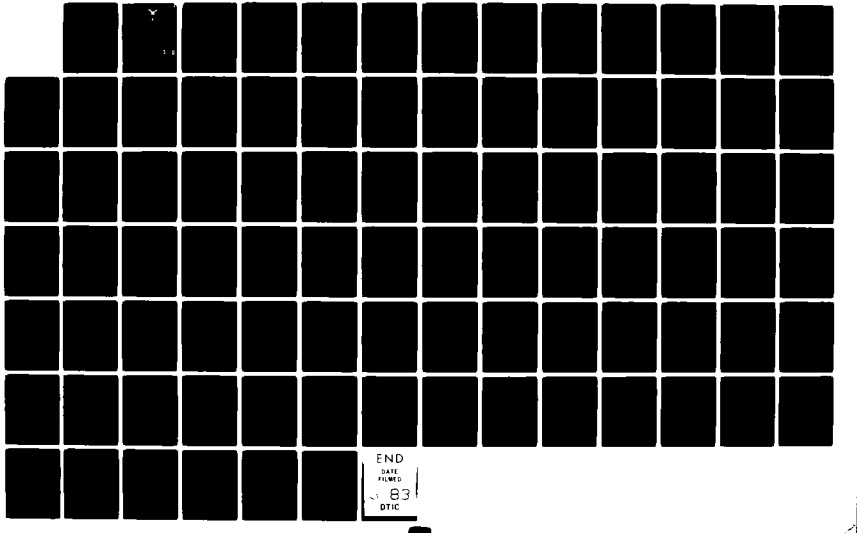

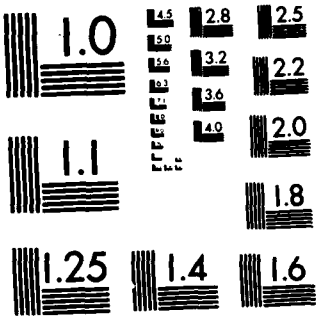

DEPARTMENT OF THE AIR FORCE
AIR UNIVERSITY (ATC)

AIR FORCE INSTITUTE OF TECHNOLOGY

Wright-Patterson Air Force Base, Ohio

MODAL CONTROL OF A SATELLITE IN AN UNSTABLE ORBIT ABOUT L3

THESIS

Frank M. DeArmond
AFIT/GAE/AA/82D-7 Capt. USAF

AFIT/GAE/AA/82D-7

MODAL CONTROL OF A SATELLITE IN AN UNSTABLE ORBIT ABOUT L3

THESIS

Presented to the Faculty of the School of Engineering
of the Air Force Institute of Technology
Air University
in Partial Fulfillment of the
Requirements for the Degree
Master of Science

by

Frank M. DeArmond, B.S.
Captain USAF

Graduate Aeronautical Engineering

December 1982

Approved for public release; distribution unlimited

Acknowledgements

I would like to express my sincere appreciation to and admiration for Dr. Bill Wiesel. His encouragement, patience and knowledge were unbounded throughout the course of this study. I will always remember him as a man of great abilities.

A debt of gratitude also goes out to Dr. Bob Calico, Dr. James Silverhorn, and Dr. Lynn Wolaver. Their teachings enlightened me in the many areas necessary to complete this work.

I also owe a great deal to Capt. Carl Wolf, and many of my fellow students. Our numerous discussions have helped overcome obstacles along the course of this study.

Finally, I would like to thank my parents and family. Without their continual love and support, this would never have been.

Table of Contents

List of Figures

List of Tables

List of Symbols

$\bar{A}$	average control of acceleration
A	coefficient matrix of variational system
B	control matrix
C	Monodromy matrix
C.T.	control term
$\bar{E}$	eigenvectors of the four-body system
e	exponentiation
G	universal gravitational constant
H	Hamiltonian of the four-body system
$\mathcal{H}$	Hessian matrix
I	identity matrix
J	Jordan form of the matrix of Poincare exponents
K	controller gain
L1-L5	Lagrange points of equilibrium in earth-moon system
Λ	matrix of eigenvectors
λ	Poincare exponents of four-body system
M	sum of the masses of the earth, moon, and sun
m_1	mass of the earth
m_2	mass of the moon
m_3	mass of the sun
$\bar{\eta}$	modal vector of the four-body problem
$\bar{\eta}_P$	forced modal vector of the four-body problem
$\bar{\eta}_F$	free modal vector of the four-body problem
p_x, p_y, p_z	momenta of the satellite

$\bar{\Phi}$	state transition matrix
$\bar{\phi}$	column vector of state transition matrix
q_x, q_y, q_z	coordinates of the satellite position
$\bar{R}$	vector from the earth-moon center of mass to the satellite
$\bar{r}$	vector from the earth to the moon
$\bar{r}_{SAT}$	inertial position vector of the satellite
$\bar{\rho}$	vector from the earth-moon center of mass to the sun
$\dot{\bar{\rho}}$	time derivative of $\bar{\rho}$ taken with respect to the rotating reference frame
t	time
t_o	initial time
T	period of orbit about L3
$\bar{u}$	control vector
ΔV	delta in velocity
$\bar{v}_{SAT}$	velocity vector of the satellite
ω	angular velocity vector of the rotating reference frame
$\bar{X}$	state vector of the four-body system
$\bar{X}_{p.o.}$	state vector along reference orbit about L3
$\delta\bar{x}$	variational state vector
$\delta\bar{x}_F$	free variational state vector
$\delta\bar{x}_p$	forced variational state vector
Z	skew-symmetrical matrix

Lagrange point 3

Abstract

A perturbation analysis was done on a satellite in orbit about L3. A modal control scheme for linear systems was then applied to the linear and nonlinear perturbations. Rectification of the satellite orbit was achieved by Encke's Method. The effects of the moon's inclination and eccentricity on the orbit stability was investigated. The controller stabilized the linear and nonlinear perturbations, with the average control acceleration being of the same order of magnitude as that for earth-synchronous satellites.

MODAL CONTROL OF A SATELLITE IN AN UNSTABLE ORBIT ABOUT L3

I. Introduction

Background

The need for total global reconnaisance via sensor bearing satellites has been obvious since Sputnik I. Equatorial synchronous satellites provide only partial coverage, not being able to "see" polar activities. Synchronous satellites also require station keeping devices, e.g. reaction jets, since they are in an inherently unstable orbit (ref. 1). The cost of this control in terms of weight may be excessive, to the point of jeopardizing the basic mission of the satellite. If a satellite can be put into an unstable orbit and kept there with a minimum amount of control, then less weight need be allocated to the control system. Therefore, the need of minimizing control requirements becomes clear. There also arises the need for a point or points in space in which a satellite can be placed and stabilized with a minimum of control cost and be able to provide total global coverage.

There are points in space where an object, when placed, will tend to remain if left unperturbed. In the Earth-Moon system these points are known as Lagrangian points L1 through L5 (See Figure 1). These points arise in the Earth-Moon system for the restricted three-body problem.

The model is such that the Earth and Moon rotate about their barycenter in circular, planar orbits. The collinear points L1, L2, and L3 are inherently unstable, and an object placed at these points, when perturbed, will tend to leave the vacinity of these points. The points L4 and L5 are inherently stable and an object placed at these points will tend to remain even if perturbed. But when a fourth body is considered, the sun, all these points become unstable.

It is known that periodic orbits about these equilibrium points exist (ref. 2). In the restricted three-body problem, if the ratio of the two larger masses is less the 1/27, orbits about the triangular points can be shown to be unstable (ref. 3). Wiesel, in an earlier work, established an orbit about L3 for the restricted four-body problem (ref. 2). Figure 2 shows this orbit. This orbit is found to be unstable. Therefore, a means must be found of stabilizing a satellite placed in this orbit.

The Lagrange points lie in the Earth-Moon plane and not the equatorial plane which makes polar reconnaisance from a satellite in orbit about L3, L4, and L5 possible. It is the lack of total global coverage by Earth synchronous satellites that makes the prospect of putting one satellite in orbit about each of the Lagrangian points L3, L4, and L5 desirable. However, it must be done such that control costs are not excessive.

Problem and Scope

In an earlier work, Shelton developed a modal control scheme for time periodic linear systems (ref. 4). This scheme was then applied to a satellite in an unstable orbit about the Earth-Moon Lagrange point L3. With the controller operating, the orbit becomes a stable reference solution (trajectory) and classical perturbation techniques could be used. Shelton's controller was designed based on a model which neglected the free lunar eccentricity, lunar inclination, and the eccentricity of the sun. When these effects, particularly the free lunar eccentricity, were included in the model, the controller could no longer stabilize the orbit.

Using Shelton's periodic orbit as a stable reference solution, Ehrler (ref. 5) did a first order perturbation analysis of the effect of the free lunar eccentricity. With the model changed to include the Moon's free lunar eccentricity, Shelton's controller responded to both the original instability, which it had previously stabilized, and the purely oscillatory linearized perturbation from the free lunar eccentricity, which in combination it could not stablize. This led to Ehrler splitting the perturbation solution into its free (homogeneous) and forced (particular) solutions which is the basic theory of linear differential equations with a forcing function. Ehrler then modified the controller to suppress only the "free" components causing

the original instability. However, when the Moon's eccentricity was included in the system model, the perturbation was so large it drove the satellite outside the linearized region the controller was designed for, rendering it unstable.

Instead of linearizing the perturbation equation, we can choose to redefine the perturbation so that it is split into two parts, the first consisting of the original instability (linearized and controllable), and the second consisting of the perturbation from the free linear eccentricity and the nonlinear terms of the original instability. By subtracting off the second part from the total perturbation we can modify the controller to suppress only the free component. This will hopefully be successful in stablizing the satellite in the reference periodic orbit, even if the perturbation is so large as to drive it outside of the linear range of the controller design. This is the goal of this study.

II. Problem Analysis

Coordinate System

The coordinate system used is shown in Figure 3. The coordinate system rotates with the same angular velocity of the moon. The origin of the system is located at the center of mass of the Earth-Moon system, the barycenter.

Dynamics

In an earlier work, Wiesel developed the dynamics for the restricted four-body problem (ref. 2). The Hamiltonian was found to be

$$H = \tfrac{1}{2}(p_x^2 + p_y^2 + p_z^2) + (p_x R_y - p_y R_x) + \frac{m_3}{M} p_x(\dot{r}_{\rho x} - \omega_{\rho y}) + p_y(\dot{r}_{\rho y} + \omega_{\rho x}) \qquad (1)$$

$$- \frac{Gm_3}{\left|(\bar{R}-\bar{\rho})\right|} - \frac{Gm_1}{\left|\frac{m_2}{m_1+m_2}\bar{r}+\bar{R}\right|} - \frac{Gm_2}{\left|\bar{R} - \frac{m_1}{m_1+m_2}\bar{r}\right|}$$

The standard units and conventions of the restricted three-body problem have been adopted here (See Appendix A).

Equations of Motion and Equations of Variation

The state vector formulated is

$$\bar{X} = \begin{bmatrix} q_i \\ p_i \end{bmatrix} \qquad i = 1, 2, \ldots n \qquad (2)$$

Where the q_i's represent the generalized coordinate and the p_i's the associated conjugate momenta in the rotating Earth-Moon frame. The equations of motion are found from Hamilton's equation

$$q_i = \frac{\partial H}{\partial p_i} \qquad p_i = -\frac{\partial H}{\partial q_i} \tag{3}$$

This can be put into the form $\dot{\bar{X}} = [Z]\,\bar{\nabla}H$ (4)

where Z is a skew-symmetric 2nx2n matrix, n being the number of degrees of freedom. Z is of the form;

$$[Z] = \begin{bmatrix} [o] & [1n] \\ [-1n] & [o] \end{bmatrix} \tag{5}$$

Here [1n] is the nxn unit matrix.

In a similar manner the equations of variation can be found from

$$\dot{\delta\bar{x}} = [Z]\,[\mathcal{H}]\,\delta\bar{x} \tag{6}$$

Where $[\mathcal{H}]$ is the 2nx2n Hessian matrix whose elements are

$$\mathcal{H}_{ij} = \frac{\partial^2 H}{\partial x_i \partial x_j} \qquad i,j = 1,\ 2n$$

(ref. 6:230).

We can put these time periodic variational equations in the form

$$\dot{\delta\bar{x}} = A(t)\ \delta\bar{x} \tag{7}$$

The periodicity is contained in the coeffiecient matrix A(t) such that

$A(t) = A(t + T)$ where T is the period of the system.

III. Floquet Solution For Periodic Systems

For a time periodic system such as

$$\dot{\delta\bar{x}} = A(t)\delta\bar{x} \tag{8}$$

There is a fundamental matrix or state transition matrix $\bar{\bar{\Phi}}(t, t_o)$, such that

$$\delta\bar{x}(t) = \bar{\bar{\Phi}}(t, 0)\ \delta\bar{x}(0) \tag{9}$$

The fundamental matrix is a function of only the initial and final times and has the property

$$\bar{\bar{\Phi}}(t, t_o) = \bar{\bar{\Phi}}(t, t_1)\ \bar{\bar{\Phi}}(t_1, t_o)$$

The n columns of $\bar{\bar{\Phi}}(t, t_o)$ each satisfy the differential equation

$$\dot{\bar{\phi}}(t) = A(t)\bar{\phi}(t) \tag{10}$$

If $\bar{\bar{\Phi}}(t_o, t_o)$ is the identity matrix, i.e.

$$\bar{\bar{\Phi}}(t_o, t_o) = I$$

Then $\bar{\bar{\Phi}}(t, t_o)$ is the principal fundamental matrix.
Floquet Theory states that

$$\bar{\bar{\Phi}}(t, T) = \bar{\bar{\Phi}}(t)C \tag{11}$$

where C is the monodromy matrix. Substituting t = 0 into Equation (11) we see that $\bar{\bar{\Phi}}(T) = C$ (12)

By investigating $\underline{\Phi}(T)$ we obtain the eigenvalues and eigenvectors at t = 0. We can obtain $\underline{\Phi}(T)$ by using appropriate initial conditions and integrating Equation (10) for n columns of $\underline{\Phi}$, over the period T. Floquet's Theory states that the general solution of Equation (8) is of the form

$$\delta\bar{x}(t) = \sum_{j=1}^{n} \beta_j \bar{E}_j(t) e^{\lambda_j t} \tag{13}$$

where β_j and λ_j are constants and the $\bar{E}_j$ are periodic functions with periodic (T). The n λ_j can be arranged in a matrix of Jordan canonical form, i.e.

$$J = \begin{bmatrix} \lambda_1 & & & \\ & \ddots & & \\ & & & \lambda_n \end{bmatrix} \tag{14}$$

(ref. 9).

The λ_j are called the characteristic exponent or Poincare Exponent and the quantity $e^{\lambda_j t}$ termed a characteristic multiplier of A(t).

In order to compute $\bar{E}_j$ and λ_j Shelton assumed that he needed to excite one mode of the system described by (8). Letting $\beta_j = 0$ for $j \neq i$ and $\beta_i = 1$ for $i = j$ from (13), we get,

$$\delta\bar{x}(t) = \bar{E}_i(t) e^{\lambda_i t} \tag{15}$$

Equating (9) and (15) we obtain

$$\bar{E}_i(t)\, e^{\lambda_i t} = \underline{\Phi}(t, 0)\,\delta\bar{x}(0) \tag{16}$$

$$= \underline{\Phi}(t, 0)\, \bar{E}_i(0) \tag{17}$$

$\bar{E}_i(t)$ is periodic

Hence $\bar{E}(T) = \bar{E}_i(0)$, which results in

$$\delta\bar{x}(T) = \bar{E}_i(T)\, e^{\lambda_i T} \tag{18}$$

$$= \bar{E}_i(0)\, e^{\lambda_i T} = \underline{\Phi}(t, 0)\, \bar{E}_i(0) \tag{19}$$

This leads to the eigenvalue problem

$$\{\underline{\Phi}(T, 0) - (e^{\lambda_i(T)})I\}\, \bar{E}_i(0) = \bar{0} \tag{20}$$

Here we see that the monodromy matrix has eigenvalues $e^{\lambda T}$ and its eigenvectors are $\bar{E}_i(0)$. To obtain the complete solution, $\bar{E}_i(t)$ must be computed over the period. Determining $\bar{E}_i(t)$ over one period determines $\bar{E}_i(t)$ for all time. Letting $t_o = 0$, Floquet's Theorem also states that we can describe the fundamental matrix, $\underline{\Phi}(t, 0)$, as

$$\underline{\Phi}(t,o) = \underline{\Lambda}(t)e^{Jt}\underline{\Lambda}^{-1}(0) \tag{21}$$

where $\underline{\Lambda}$ is the matrix of eigenvectors

$$\underline{\Lambda}(t) = [\bar{E}_1(t), \bar{E}_2(t) \ldots \bar{E}_n(t)] \tag{22}$$

and is such that $\underline{\Lambda}(T) = \underline{\Lambda}(0)$, i.e., the eigenvectors

are periodic. For the control analysis we will need the eigenvectors around the periodic orbit about L_3 (ref. 7). Using Equation (10) and Equation (21), we get

$$A(t)\underline{\Phi}(t) = A(t)\underline{\Lambda}(t)e^{Jt}\underline{\Lambda}^{-1}(0) \tag{23}$$

differentiating (21) leads to

$$\dot{\underline{\Lambda}}e^{Jt}\underline{\Lambda}^{-1}(0) + \underline{\Lambda}Je^{Jt}\underline{\Lambda}^{-1}(0) = A(t)\underline{\Phi} \tag{24}$$

$$= A\underline{\Lambda}(t)e^{Jt}\underline{\Lambda}^{-1}(0) \tag{25}$$

This simplifies to

$$\dot{\underline{\Lambda}}(t) = A(t)\underline{\Lambda}(t) - \underline{\Lambda}(t)J \tag{26}$$

This is the equation that, when integrated, gives the eigenvectors around the periodic orbit.

The Floquet Theory described above was used to investigate the stability of the orbit about L3. The orbit was found to be unstable since one of the system's Poincare exponents is a positive real root, while its conjugate is negative. The remaining exponents are purely imaginary.

Table I

Poincare Exponents of L3 Periodic Orbit

Mode	Poincare Exponent
Planar	0.0+0.77738i
	0.0-0.77738i
Planar	0.17893+0.0i
	-0.17893+0.0i
Out of Plane	0.0+0.84134i
	0.0-0.84134i

In Shelton's orbit, the unstable exponent was designated λ_3 and is the root that his controller affected. Implementing the controller yields

$$\dot{\delta\bar{x}} = A(T)\delta\bar{X}(T) + B(t)\bar{u}(t) \tag{27}$$

where $\bar{u}(t)$ is the control vector and B(t) is the control matrix. Since it is only desired for the controller to affect only one mode, it is necessary to uncouple the modes. This can be done by a similarity transformation (ref. 8:170-172). Defining the uncoupled variable vector as $\bar{\eta}(t)$, we can obtain $\bar{\eta}(t)$ from

$$\bar{\eta}(t) = \Lambda^{-1}(t)\ \delta\bar{x}(t) \tag{28}$$

where Λ^{-1} is the inverse of the eigenvector defined in (22). Differentiating Equation (28) with respect to time yields

$$\dot{\delta\bar{x}} = \dot{\Lambda}(t)\bar{\eta}(t) + \Lambda(t)\dot{\bar{\eta}}(t) \tag{29}$$

In order to obtain a differential equation for the modal coordinates, equate Equations (27 and (28) to get

$$\dot{\bar{\eta}} = \Lambda^{-1}(t)\,[A(t)\Lambda(t) - \dot{\Lambda}(t)]\,\eta(t) + \eta^{-1}(t)B(t)\bar{u}(t) \qquad (30)$$

From (26) we had

$$\dot{\Lambda} = A(t)\,\Lambda(t) - \Lambda(t)J$$

substituting into (30) yields

$$\dot{\bar{\eta}} = J\bar{\eta} + \Lambda^{-1}(t)B(t)\bar{u}(t) \qquad (31)$$

Since the system is diagonalized, it is now a relatively simple task to feed back the single unstable mode. This is the method of modal control. Since λ_3 was designed as the unstable exponent, this requires that $\bar{u} = k\eta_3$. This yields

$$\dot{\bar{\eta}} = J\bar{\eta} + \Lambda^{-1}(t)B(t)K\eta_3 \qquad (32)$$

IV. Perturbation Analysis

Development of Perturbations

In the restricted four-body problem, i.e. no inclination or eccentricity of the moon is included, the perturbation from the reference periodic orbit becomes

$$\delta\bar{x}_F = \bar{X} - \bar{X}_{p.o.} \tag{33}$$

where X are the actual states and $\bar{X}_{p.o.}$ are the states of the reference periodic orbit. The $\delta\bar{x}_F$ designates that this is a free perturbation, i.e. no forcing function from the Moon's eccentricity or inclination. Shelton found this is an unstable yet controllable system with

$$\dot{\delta\bar{x}}_F = A(t)\ \delta\bar{x}_F \tag{34}$$

This is also a linearized system, Since second order terms and higher were truncated.

In the unrestricted four-body problem the Moon's eccentricity and inclination must be included. Choosing to define the perturbation

$$\delta\bar{x} = \delta\bar{x}_F + \delta\bar{x}_p \tag{35}$$

where $\delta\bar{x}_F$ is defined as in (33) it is seen that $\delta\bar{x}_p$ must include the perturbation due to the forcing function from the Moon's eccentricity, inclination and any nonlinear terms not included in the restricted four-body problem. It should be noted the instabilities in the restricted four-body problem arise from the linearized forcing terms due to the

inclusion of the sun. Therefore, the nonlinear terms in the unrestricted four-body problem are the nonlinear part of the forcing function from the inclusion of the sun in the system model.

Since the total perturbation is derived as

$$\delta\bar{x} = \bar{X}_R - \bar{X}_{p.o.} \tag{36}$$

where $\bar{X}_R$ are the states in the unrestricted model, by equating (35) and (36) it is seen that

$$\delta\bar{x}_F = \bar{X}_R - \bar{X}_{p.o.} - \delta\bar{x}_p \tag{37}$$

substituting (37) into (34)

$$\delta\dot{\bar{x}}_F = A(t)\ [\bar{X}_R - \bar{X}_{p.o.} - \delta\bar{x}_p] \tag{38}$$

rearranging (35) yields

$$\delta\bar{x}_p = \delta\bar{x} - \delta\bar{x}_F \tag{39}$$

substituting (35) gives

$$\delta\bar{x}_p = \bar{X}_R - \bar{X}_{p.o.} - \delta\bar{x}_F \tag{40}$$

Time differentiating (40) and substituting (38) produces

$$\delta\dot{\bar{x}}_p = \dot{\bar{X}}_R - \dot{\bar{X}}_{p.o.} - A(t)[\bar{X}_R - \bar{X}_{p.o.} - \delta\bar{x}_p] \tag{41}$$

which is an explicit differential equation for the nonlinear perturbation.

Perturbation Verification

To insure that the states and perturbations were being calculated correctly, a check was done by comparing the states derived from the total nonlinear equations of motion with those derived from Equations (4), (37), and (41). This was done in the following manner:

$$\bar{X}_R(t) = \bar{X}_{p.o.}(t) + \delta\bar{x}_p(t) + \delta\bar{x}_F \tag{42}$$

But from Equations (8), (9), and (23)

$$\delta\bar{x}_F(t) = \underline{\Lambda}(t)\, e^{Jt}\, \underline{\Lambda}^{-1}(0)\, \delta\bar{x}_F(0) \tag{43}$$

which gives

$$\bar{X}_R(t) = \bar{X}_{p.o.}(t) + \underline{\Lambda}(t)e^{Jt}\ \underline{\Lambda}^{-1}(0)\ \delta\bar{x}_F(0)$$

$$+ \delta\bar{x}_p(t) \tag{44}$$

using Equations (4), (37), and (41) for $\dot{\bar{X}}_{p.o.}(t)$, $\delta\bar{x}_F$ and $\delta\dot{\bar{x}}_p(t)$, respectively, and integrating (4) and (41), the state vector $\bar{X}_R$ was calculated. This state vector was checked against the state vector derived from the nonlinear equations of motion, (4), and was found to agree extremely well. This verified the states and perturbations were being calculated correctly.

With Equations (34) and (41) the controller can now be implemented in such a way as to affect only the original instabilities which manifest themselves in $\delta\bar{x}_F$,

and by ignoring those arising in $\delta\bar{x}_p$, which if they remain small, are of no consequence and can be ignored. In this way the system can be stabilized in the "real" dynamics of the complete unrestricted four-body problem. However, to insure non-excitement of the stable modes, the controller must be implemented in the diagonalized, uncoupled modal coordinate system.

V. Development of the Controller

Control Term Derivation

It is desired to control only the "free" part of the perturbation $\delta\bar{x}_F$, but this must be done in the modal coordinate system to insure non-excitement of the stable modes.

We must first insure that the modal coordinates can be split into their forced and free components, as the perturbations are in Equation (35). Equating (35) and (28) produces

$$\Lambda\bar{\eta} = \delta\bar{x}_p + \delta\bar{x}_F \tag{45}$$

or

$$\bar{\eta} = \Lambda^{-1}\,\delta\bar{x}_p + \Lambda^{-1}\delta\bar{x}_F \tag{46}$$

defining

$$\Lambda^{-1}\,\delta\bar{x}_p = \bar{\eta}_p \tag{47}$$

and $\Lambda^{-1}\,\delta\bar{x}_F = \bar{\eta}_F$

Equation (43) becomes

$$\bar{\eta} = \bar{\eta}_p + \bar{\eta}_F \tag{48}$$

and it is seen that the modal coordinate can be defined in the same manner as Equation (35).

Differentiating the free part of Equation (47) yields

$$\dot{\delta\bar{x}}_F = \Lambda\dot{\bar{\eta}}_F + \dot{\Lambda}\bar{\eta}_F \tag{49}$$

Equating this to Equation (27)

$$\dot{\delta\bar{x}}_F = \Lambda\dot{\bar{\eta}}_F + \dot{\Lambda}\bar{\eta}_F \tag{50}$$

$$= A(t)\ \delta\bar{x}_F(t) + B(t)\bar{u}(t)$$

and solving for $\dot{\bar{\eta}}_F$

$$\dot{\bar{\eta}}_F = \Lambda^{-1}(t)\ [A(t)\ \Lambda(t) - \dot{\Lambda}(T)]\bar{\eta}_F + \Lambda^{-1}B(t)\bar{u}(t) \tag{51}$$

from (26) and (32)
is obtained

$$\dot{\bar{\eta}}_F = J\bar{\eta}_F + \Lambda^{-1}(t)\ B(t)\ K\bar{u} \tag{52}$$

where $\bar{u} = K\eta_3$ and K is the control gain. The
B matrix defined such that $B_3 = [0,\ 1.,\ 0,\ 1.,\ 0,\ 0]^T$ (53)
where 3 designates the third column, which is the same as used in previous studies. The other 5 columns are zero. This corresponds to two fixed thrusters operating at a 45° angle to the Earth-Moon line.

In a similar manner the equation of motion for the forced perturbation can be found to be

$$\dot{\bar{\eta}}_p = \Lambda^{-1}(t)\,[\dot{\bar{X}}_R - \bar{X}_{p.o.} - A(t)\,\delta\bar{x}_F]$$

$$- \Lambda^{-1}(t)\,[A(t)\Lambda(t) - \dot{\Lambda}(t)J]\,\bar{\eta}_p \qquad (54)$$

It is necessary to implement the controller in the real system model, since a controller can only affect the "real world" dynamics. In the most general sense, the control vector is $\bar{u} = K\bar{\eta}_F$, (55)

substituting for $\bar{\eta}_F$ from Equation (28)

$$\bar{u} = K\,\Lambda^{-1}(t)\delta\bar{x}_F(t) \qquad (56)$$

The control term which is added to the equations of motion (4) becomes

$$C.T. = B\bar{u}$$

$$= B\,K\,\Lambda^{-1}(t)\,\delta\bar{x}_F(t) \qquad (57)$$

using the definition for $\delta\bar{x}_F$ of Equation (37), the control term becomes

$$C.T. = B\,K\,\Lambda^{-1}(t)\,[\bar{X}_R - \bar{X}_{p.o.} - \delta\bar{x}_p] \qquad (58)$$

Now, integrating Equation (41), and choosing initial conditions for $\delta\bar{x}_p$, the control term can be calculated around the orbit and added to the equations of motion (4).

Calculation of Controller Gain

Equation (31) can be expanded to

$$\begin{bmatrix} \dot{\eta}_1 \\ \dot{\eta}_2 \\ \dot{\eta}_3 \\ \dot{\eta}_4 \\ \dot{\eta}_5 \\ \dot{\eta}_6 \end{bmatrix} = \begin{bmatrix} \lambda_1 & & & & & \\ & \lambda_2 & & [0] & & \\ & & \lambda_3 & & & \\ & & & \lambda_4 & & \\ & [0] & & & \lambda_5 & \\ & & & & & \lambda_6 \end{bmatrix} \begin{bmatrix} \eta_1 \\ \eta_2 \\ \eta_3 \\ \eta_4 \\ \eta_5 \\ \eta_6 \end{bmatrix} + \Lambda^{-1} B\bar{u} \qquad (59)$$

Since the third modal coordinate has been designated as the unstable mode, we wish to feed back η_3. This resulted in choosing

$$\bar{u} = K \eta_3 \qquad (60)$$

The B matrix is chosen to be a constant matrix and is representative of the physical constraints of the problem. Since only the inertial velocity components of the satellite can be controlled, the B matrix is chosen as defined in the last section. This corresponds to two reaction jets aligned oppositely and 45° from the X-Y axes. The third modal coordinate differential equation, with the controller, now becomes

$$\dot{\eta}_3 = [\lambda_3 + K\bar{e}(t)] \eta_3 \qquad (61)$$

where

$$\bar{\epsilon} = \Lambda^{-1}(t)\bar{B} \tag{62}$$

Equation (57) can be solved using an integrating factor. $\bar{e}$ is available as a Fourier Series. Separating e_3 into its constant and sinusoidal parts, the solution to (61) is

$$\eta_3(t) = \eta_3(0)\exp(\lambda_3 + Ke_{3C})t \exp\left[\int_o^t Ke_{3p}(t)\alpha t\right] \tag{63}$$

Since the last exponential is a periodic function of time, the equation for the new Poincare' exponent for the third mode simply becomes

$$\lambda_3' = \lambda_3 + K\,(\Lambda^{-1}_{32} + \Lambda^{-1}_{34}) \tag{64}$$

using the value for the old Poincare exponent, λ_3, and the D.C. part for Λ^{-1}_{32} and Λ^{-1}_{34}, Equation (64) becomes

$$\lambda_3' = .1789305466 - 12.96306103(K) \tag{65}$$

Using Equation (65) the gain K could be chosen to place the new Poincare' exponent, λ_3' in the stable left half plane. Choosing a new Poincare' exponent of $\lambda_3' = -.1789305466$, the gain becomes K = .027606218.

orbits, with no moon's eccentricity or inclination included and with no control i.e. K = 0, for 4 orbits. As can be seen in Figures 4 and 5 η_1 and η_2 exhibit the expected general behavior. From Figure 6 it is seen that η_3 grows exponentially as expected. However, the modes grow until they exit the region where the linearization is valid. Mode four verifies this behavior, since η_4 should decrease exponentially, which it does initially but then oscillates erratically as the linear regime is exceeded. Figures 8 through 11 show the modal coordinates versus orbits, with no control, but with eccentricity and inclination included. It is seen that the coordinates almost immediately are within the nonlinear region (note the scale difference from Figures 4-7) and hence the system is totally unstable.

To verify that the controller was working correctly, the Shelton model was duplicated and the controller applied to check and insure the model could be controlled as Shelton's controller had done. The model was duplicated by removing the nonlinear terms and inclination and eccentricity effects from the control term. This results in Equation (58) becoming

$$C.T. = B\,K\,\Lambda^{-1}\,[\bar{X}_R - \bar{X}_{p.o.}] \qquad (66)$$

which indicates that the controller is acting only on the linear perturbation terms in the restricted four-body

Evaluation of the Controller

The controller was designed based on a linearized set of equations but was applied to the full nonlinear equations of motion. Since it is required to control a satellite with all effects included, the controller was included in the full nonlinear equations which represent the most realistic model available.

From Chapter IV of this report, without the controller, it is expected that η_1 and η_2 will be purely oscillatory, η_3 will exponentially increase η_4 will exponentially decrease. The last two modes remain zero since no initial condition was given and no forces are present which will generate these components. This can be seen from Equations (14) and (31). With no control (31) becomes

$$\begin{bmatrix} \dot{\eta}_1 \\ \dot{\eta}_2 \\ \dot{\eta}_3 \\ \dot{\eta}_4 \\ \dot{\eta}_5 \\ \dot{\eta}_6 \end{bmatrix} = \begin{bmatrix} \lambda_1 & & & & & \\ & \lambda_2 & & & & \\ & & \lambda_3 & & & \\ & & & \lambda_4 & & \\ & & & & \lambda_5 & \\ & & & & & \lambda_6 \end{bmatrix} \begin{bmatrix} \eta_1 \\ \eta_2 \\ \eta_3 \\ \eta_4 \\ \eta_5 \\ \eta_6 \end{bmatrix}$$

From Table I we can see that the modal coordinates will behave as described above. Figures 4 through 7 show the modal coordinates η_1 through η_4 versus the number of

MODAL CONTROL OF A SATELLITE IN AN UNSTABLE ORBIT ABOUT L3

THESIS

AFIT/GAE/AA/82D-7

Frank M. DeArmond
Capt. USAF

problem, since the free perturbation term is defined as in Equation (37). Figures 12 through 15 show the results of this verification. Figures 12 and 13 show that modes one and two are oscillatory as expected, and Figures 14 and 15 reveal that modes three and four decrease exponentially. An exponential curve fit was done on mode three, the controlled mode. The resulting equation was

$$\eta_3 = -.229e^{-.161(t)} \tag{67}$$

The Poincare exponent for mode three is

$$P.E. = -.179$$

and it is seen that the two exponents agree well within the accuracy of the curve fit.

VI. Results, Conclusions, Recommendations

Inclusion of Nonlinear Perturbations

The next step in the control analysis was to include the nonlinear terms from the restricted four-body problem in the model, and have the controller act on not only $\delta\bar{x}_F$, but the $\delta\bar{x}_p$ as well.

The control term is defined in Equation (58) as

$$C.T. = B\ K\ \Lambda^{-1}\ [\bar{X}_r - \bar{X}_{p.o.} - \delta\bar{x}_p]$$

Figures 16 through 19 show the results of the controller acting in this model with $\delta\bar{x}_p$ included. No effects from the moon's Keplerian eccentricity or inclination have been included in this model, only the above mentioned nonlinear terms from the sun and moon's free pertubations. As can be seen in Figure 18, modal coordinate three, η_3, is diverging. When η_3 is so large as to be outside the controllable region, all the modes go unstable, as is indicated in Figure 19 by η_4 approaching zero, then diverging after approximately three orbits. A new method had to be devised to stabilize not only the free perturbation, $\delta\bar{x}_F$, but also the nonlinear perturbations.

Encke's Method

The method used in designing the controller to stablize the linear and nonlinear perturbations was Encke's Method (ref. 9: 390-396). Shelton's controller had stablized the free linear perturbations resulting in a new reference periodic orbit. Figure 20 shows this reference periodic orbit and the actual orbit the satellite would traverse. The difference between these two orbits is the perturbation caused by the nonlinear effects. In Encke's Method, when the perturbation grows larger than a specified value, rectification occurs. Rectification means that a new epoch and starting point is chosen which coincides with the actual orbit of the satellite. The controller is activated at this point to zero out the perturbation, and place the satellite back on the desired reference orbit. This results in higher control costs, but is a necessary function in order to stabilize the satellite. Rectification was achieved by zeroing out the nonlinear perturbation, which results in the controller being activated. This can be seen from Equation (58). At time of rectification, the nonlinear term, $\delta\bar{x}_p$, has grown to such a value that it is approaching in magnitude the free perturbation, $\delta\bar{x}_F$, which is defined in Equation (37). This results in the control term, Equation (58), being of small magnitude. By setting $\delta\bar{x}_p$ to zero, the controller is "turned on" and reacts to what it now "thinks" is the free perturbation.

This, in effect, "dumps" the nonlinear perturbation into the free perturbation. This "dumping" is perfectly valid because how the perturbation is split up arbitrarily and the controller reacts on the total perturbation when rectification occurs. In order to determine when to rectify, an average value of the perturbation states, i.e.

$$\left| \bar{\delta x}_{p_{avg}} \right| = \frac{\left|\delta q_x\right| + \left|\delta p_x\right| + \left|\delta q_y\right| + \left|\delta p_y\right|}{4} \qquad (68)$$

was calculated. When the value exceeded an arbitrary value, rectification occured.

Results of Encke's Method

Using the same initial conditions as were used when verifying the controller would zero out the free perturbation only, Encke's Method was used to zero out both the free perturbation and the nonlinear perturbations. Figures 21 through 24 show the results of this rectification scheme. Figure 23 reveals that the controller zeros out the initial transient and then acts as a dead band controller. Modal coordinates one and two exhibit the expected oscillatory behavior. Coordinate three, the unstable mode coordinate, demonstrates stable behavior. The periodic spikes are generated when rectification occurs, activating the controller.

Shelton had succesfully stabilized the free perturbation for approximately 2 years or 24 months. Figures 25 through 28 show the controller acting for a

period of 5 years (60 orbits). It is seen that rectification successfully stablizes the free and nonlinear perturbations for this period of time, and it appears would continue to do so for much longer periods of time. Figures 25 and 26 also show the sun's effect. This effect shows up in the one year frequency of this oscillatory mode.

The moon's eccentricity and inclination were included in the next step of the analysis. This was to determine if Encke's Method and the redefinition of the perturbation could successfully control the instabilities which arise from these lunar forcing functions. Figures 29 through 32 show the results of including inclination and eccentricity of the moon. It is seen that all the modes have gone unstable within six orbits. The perturbations grow rapidly and enter the nonlinear region almost immediately. Since the controller stablized the nonlinear terms in the restricted four-body problem, this implies that the perturbations arising from these terms do not grow at an uncontrollable rate or are merely oscillatory. However, the perturbations from the moon's inclination and eccentricity do grow at too fast a rate for the controller to handle.

It is also possible that one or both of the oscillatory modes becomes unstable with the inclusion of the Lunar inclination and eccentricity. Since the real mode is the only mode controlled, an oscillatory mode going unstable would eventually render all the mode unstable.

Control Costs

Without the Lunar inclination and eccentricity included, the controller successfully stablized the satellite, as discussed in the previous section. A limitation was put on the magnitude of the average nonlinear perturbation, $\delta\bar{x}_{p_{avg}}$, defined by (68). To analyze the effect of varying this limitation a control cost or an average control acceleration must be computed.

Since control is an acceleration (Δ velocity),

$$\Delta V = \int_o^t |\text{control acceleration}|\ dt \qquad (69)$$

where Δv is the change in velocity. An average acceleration is,

$$\bar{A} = \frac{1}{t}\int_o^t |\text{control acceleration}|\ dt \qquad (70)$$

where $\bar{A}$ is the average acceleration.

The average acceleration was calculated for several test cases. The controller must first zero out any transients in the initial values of the states and will then act as a dead band controller, allowing the satellite to drift until the maximum value of $\delta\bar{x}_{p_{avg}}$ is reached. This leads to the average acceleration being relatively large initially and then settling down to a constant value after a period of time has elapsed.

Figure 33 shows the average acceleration versus orbits, and exhibits the expected behavior. The periodic spikes are caused from rectification occuring, and the controller is activated. The average acceleration approaches a fairly constant value after 36 orbits.

An analysis was done to determine the effect of varying the limit of $\delta\bar{x}_{p_{avg}}$ on the average control cost. Runs were made for 36 orbits (3 years) and the results can be seen in Table II. If the limit on $\delta\bar{x}_{p_{avg}}$ is set too large, the control acceleration is very large, indicating that the satellite "drifts" far from the reference orbit and when rectification occurs, the controller must expend a large amount of energy to drive the perturbation to zero. As the limit on $\delta\bar{x}_{p_{avg}}$ is tightened, the average acceleration decreases as expected since the controller does not need to exceed as much energy to drive the perturbation to zero. However, the number of rectifications per orbit, which is equivilant to the number of times the controller is activated, increases slightly, as expected. Figure 34 shows

the average acceleration versus the limit on $\delta\bar{x}_{p_{avg}}$, on a log-log scale. This plot indicates the trends discussed above.

Table II

$\delta\bar{x}_{p_{avg}}{}_{max}$	$\bar{A}$	Rectification Per Orbit
1×10^{-2}	Large (10^{7})	
1×10^{-3}	$.87 \times (10^{-4})$	2.08
1×10^{-4}	$.86 \times (10^{-5})$	1.86
1×10^{-5}	$.76 \times (10^{-6})$	1.94
1×10^{-6}	$.14 \times (10^{-6})$	2.11
1×10^{-7}	$.38 \times (10^{-7})$	2.5

Recommendations

The controller demonstrated its ability to stabilize the nonlinear terms in the perturbations caused from the influences of the earth, moon, and sun. When the moon's eccentricity and inclination were included, the controller could no longer stabilize the system. The controller was derived based on modal control, and only one mode, the real unstable mode, was controlled. It is possible that the oscillatory mode becomes unstable with the inclusion of eccentricity and inclination. This would result in the

total sytem becoming unstable, since no control is placed on the oscillatory mode. It may, therefore, be necessary to place some form of control e.g. damping, on the oscillatory mode. Unfortunately, we are not free to choose what the controller may act on, since the controller can only act on the momentum components of the perturbation. A limitation is consequently placed on how the modes may be controlled. Therefore, a method must be developed that will allow placement of the individual Poincare exponents, within the physical restrictions of the problem.

Bibliography

1. Wolaver, Lynn E. Lecture Notes for MC 6.36, Advanced Astrodynamics, School of Engineering, Air Force Institute of Technology, Wright-Patterson AFB, 1982.

2. Wiesel, W. E. "The Restricted Earth-Moon-Sun Problem I: Dynamics and Libration Point Orbits," 1981.

3. Steg, L. and Devrics, J. P. "Earth-Moon Libration Points: theory, existence and Applications," Space Science Reviews, 5: 210-233 (February 1966).

4. Shelton, W. S. Modal Control of a Satellite In Orbit About L3. MS Thesis. Wright-Patterson AFB, Ohio: Air Force Institute of Technology, December, 1980.

5. Ehrler, D. N. A Perturbation Analysis of Modal Control of An Unstable Periodic Orbit. MS Thesis. Wright-Patterson AFB, Ohio: Air Force Institute of Technology, 1981.

6. Meirovitch, L. Methods of Analytical Dynamics. New York: McGraw-Hill, 1970.

7. Wiesel, W. E. and Shelton, W. L. "Modal Control of An Unstable Orbit," unpublished paper, Aire Force Institute of Technology, 1981.

8. D'Azzo, J. J. and Houpis, C. H. Linear Control System Analysis and Design. New York: McGraw-Hill, 1981.

9. Bate, R., Mueller, D., and White, J. Fundatmentals of Astrodynamics. New York: Dover Publications, 1971.

APPENDICES

Appendix A

Appendix A

$\bar{\omega}$ = Angular velocity of the rotating frame; the moon's mean inertial angular velocity vector

m_1 = mass of earth

m_2 = mass of moon

m_3 = mass of sun

G = Universal Gravitational Constant (set equal to 1)

$\frac{m_3}{M}$ = Scale factor locating the inertial point of system

Appendix B

Figures

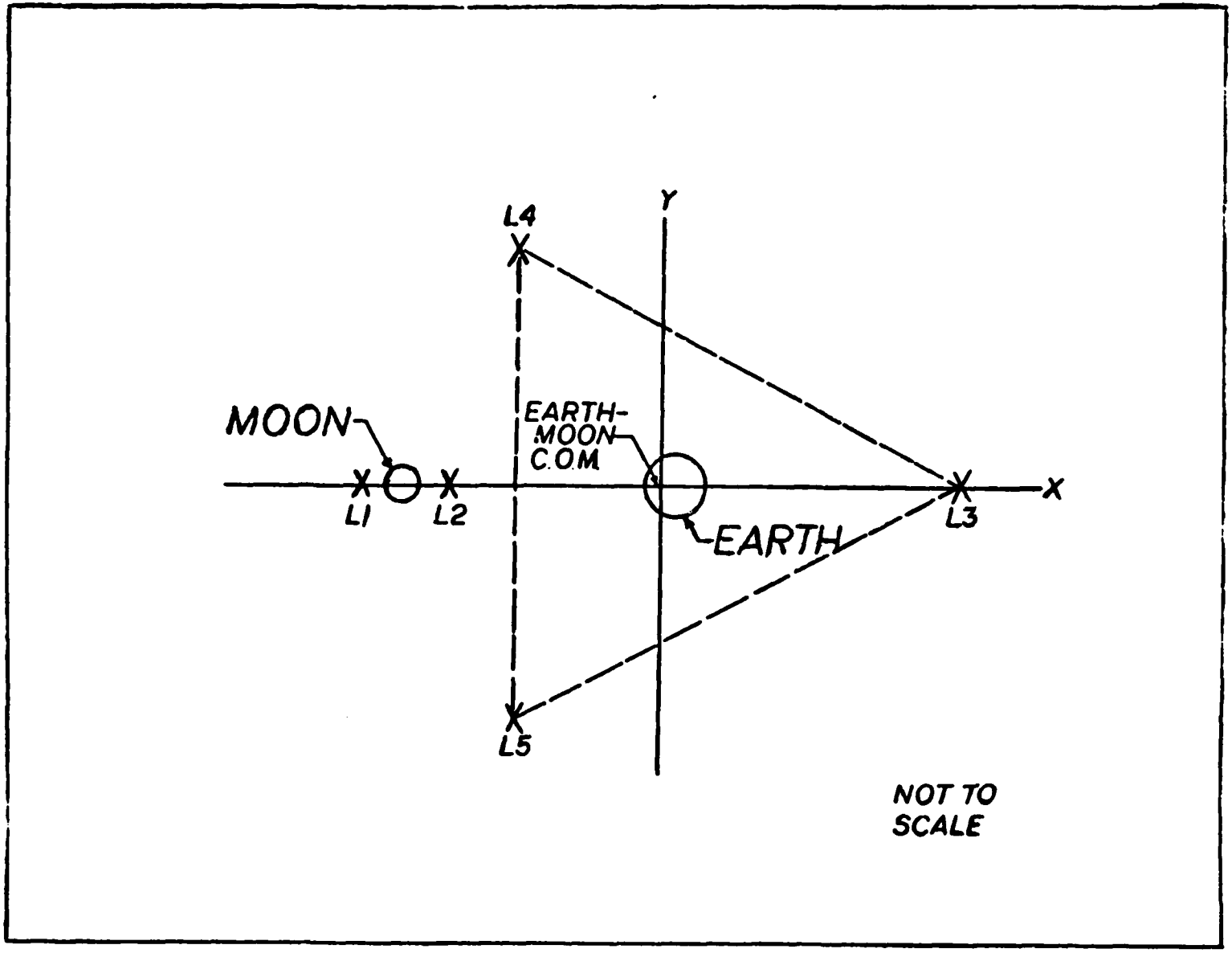

Figure 1. Lagrange Points in Earth-Moon System

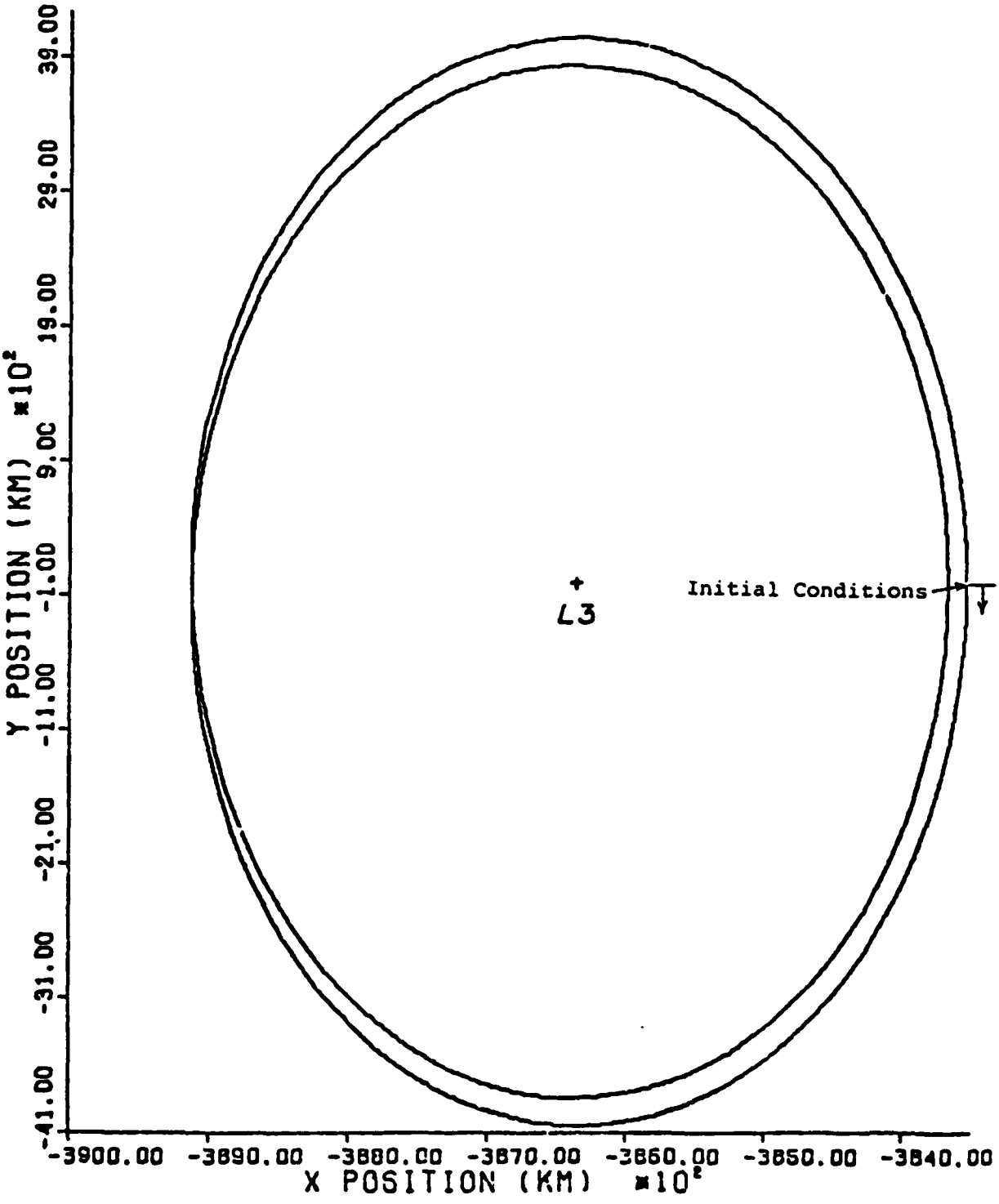

Figure 2. Wiesel Orbit About L3

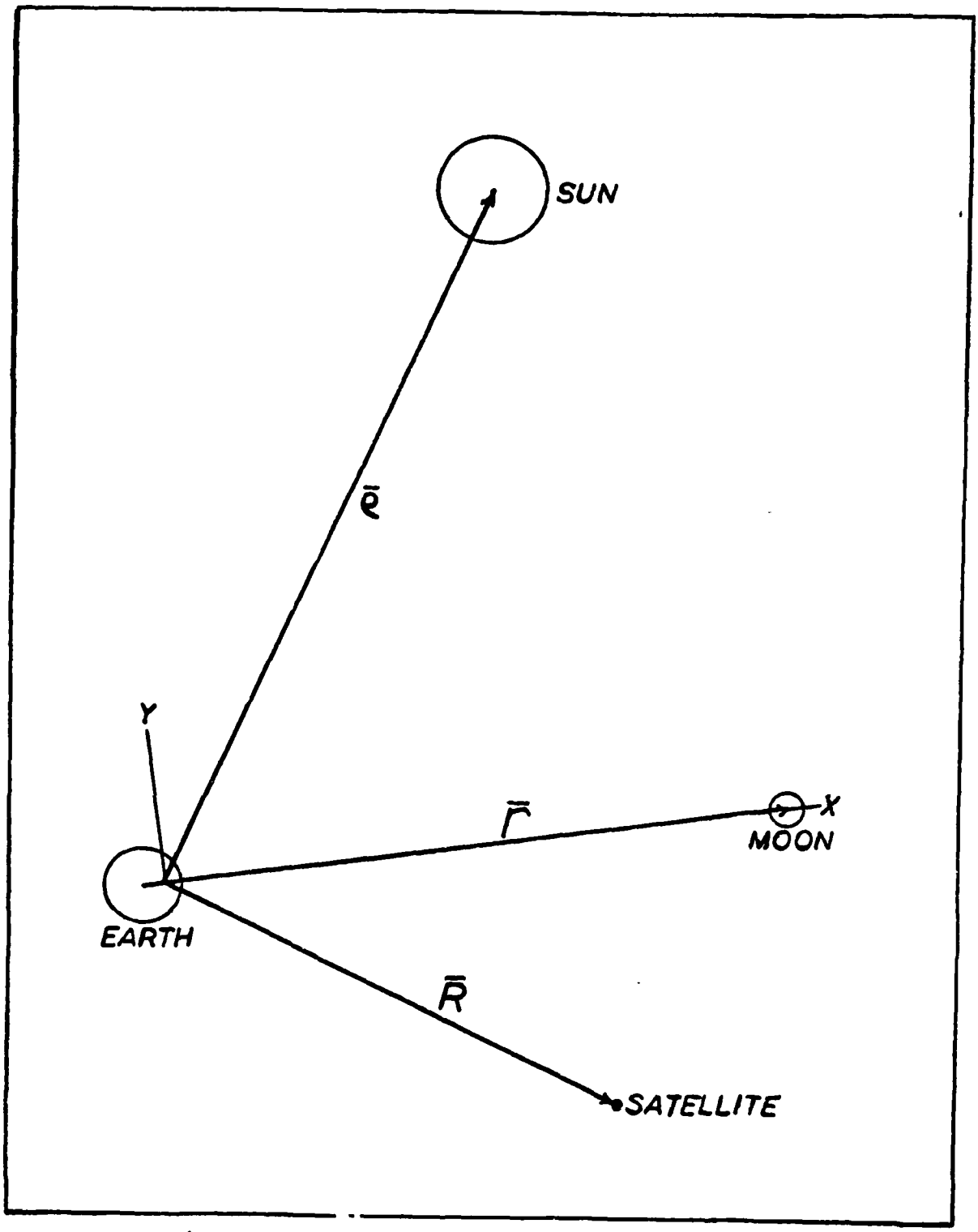

Figure 3. Geometry of the Four-Body Problem

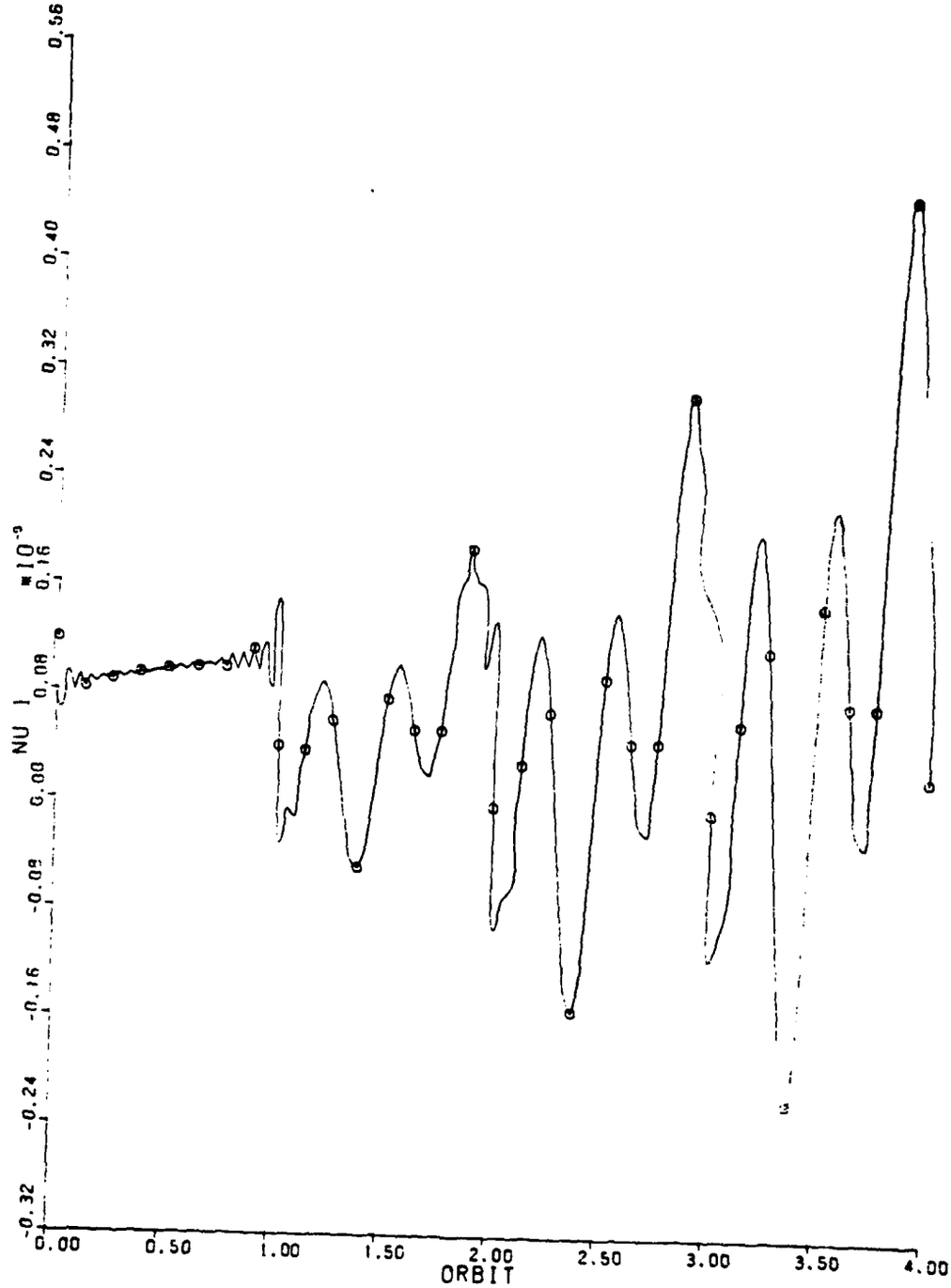

Figure 4: Modal Coordinate 1, No Eccentricity Or Inclination, ($\dot{\bar{x}}(0)=\bar{0}$, 4 Orbits)

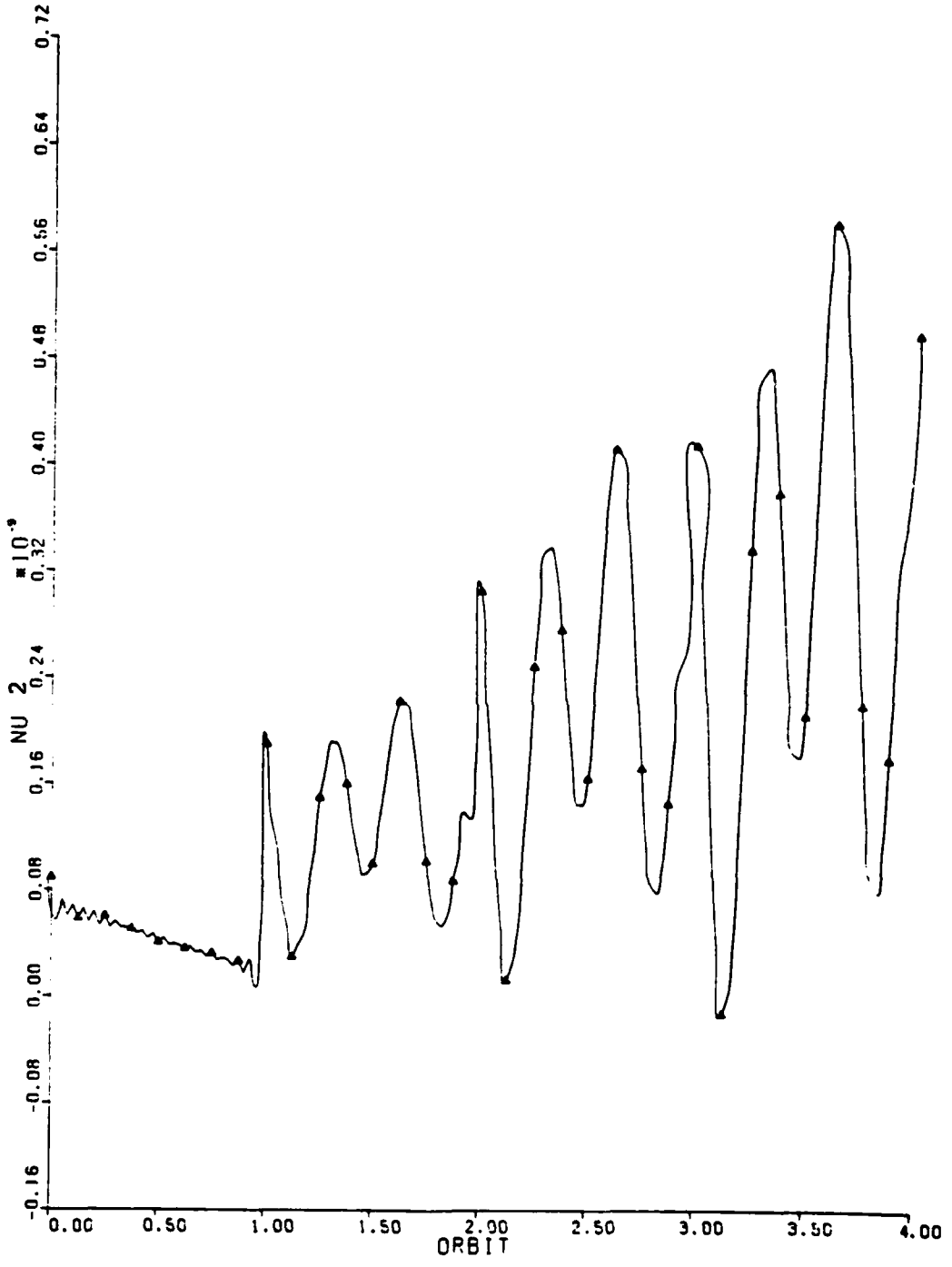

Figure 5: Modal Coordinate 2, No Eccentricity Or Inclination, ($\dot{\bar{x}}(0)=\bar{0}$, 4 Orbits)

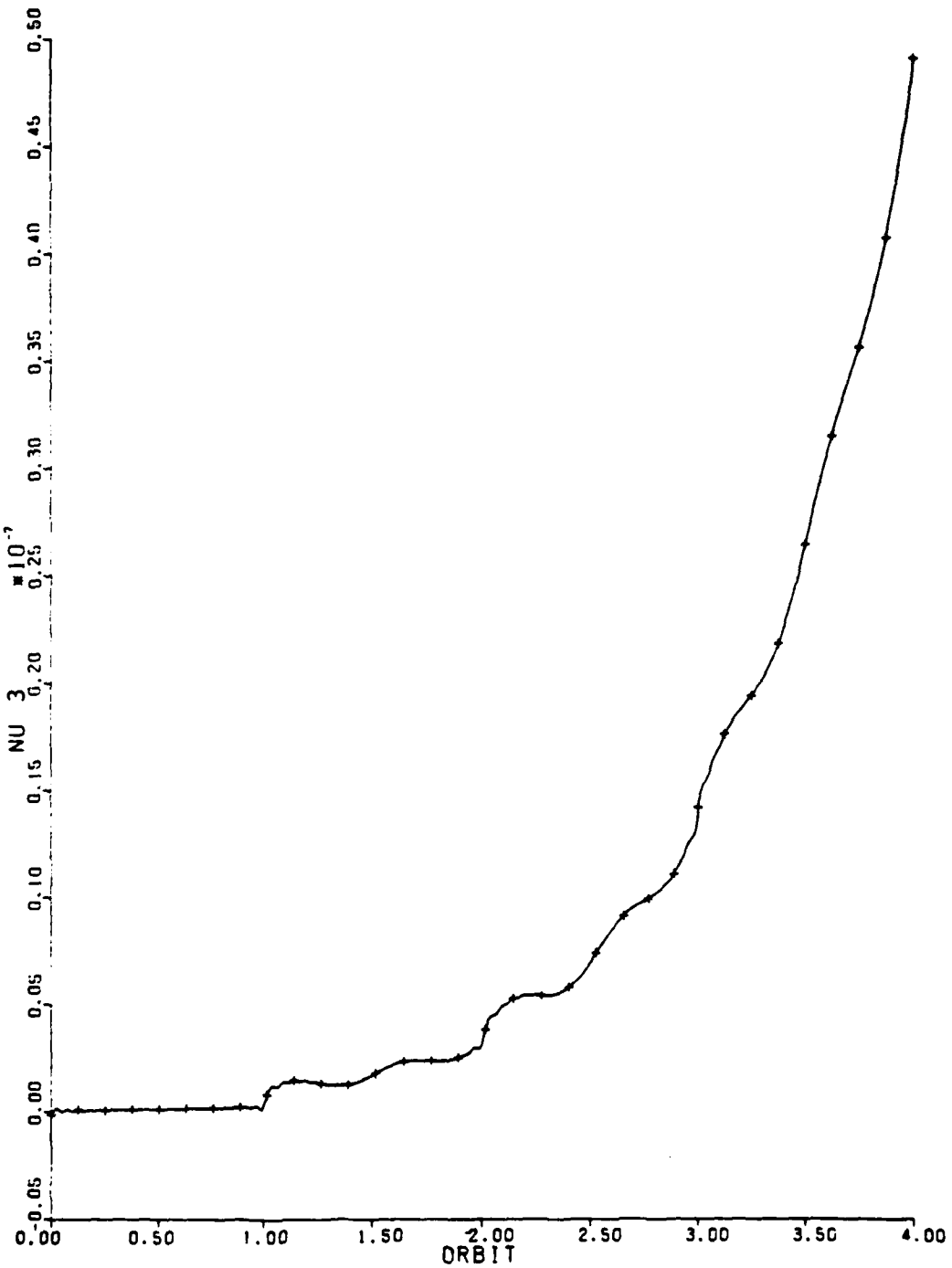

Figure 6: Modal Coordinate 3, No Eccentricity Or Inclination, ($\delta\bar{x}(0)=\bar{0}$, 4 Orbits)

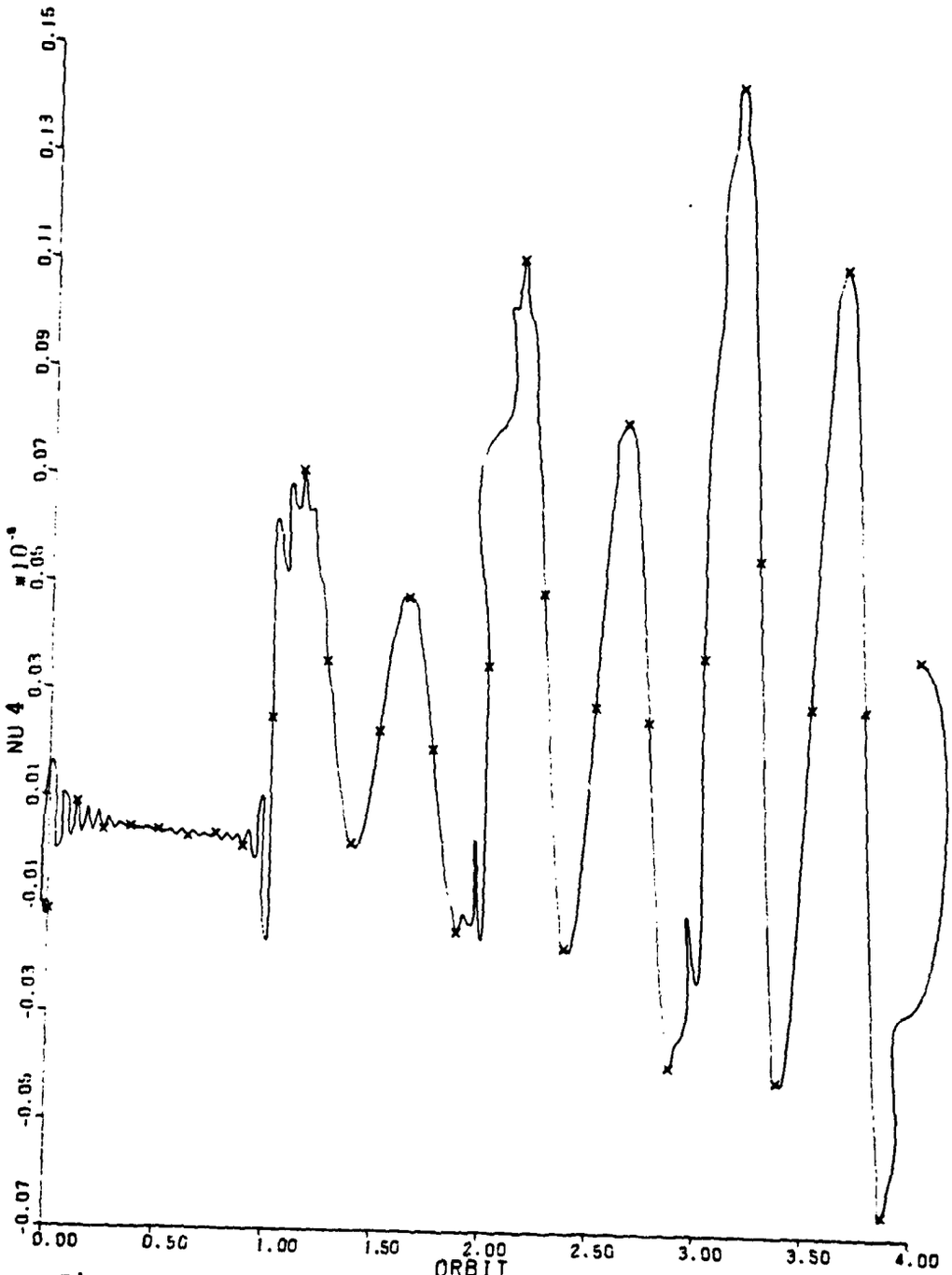

Figure 7: Modal Coordinate 4, No Eccentricity Or Inclination, ($\bar{\delta x}(0)=\bar{0}$, 4 Orbits)

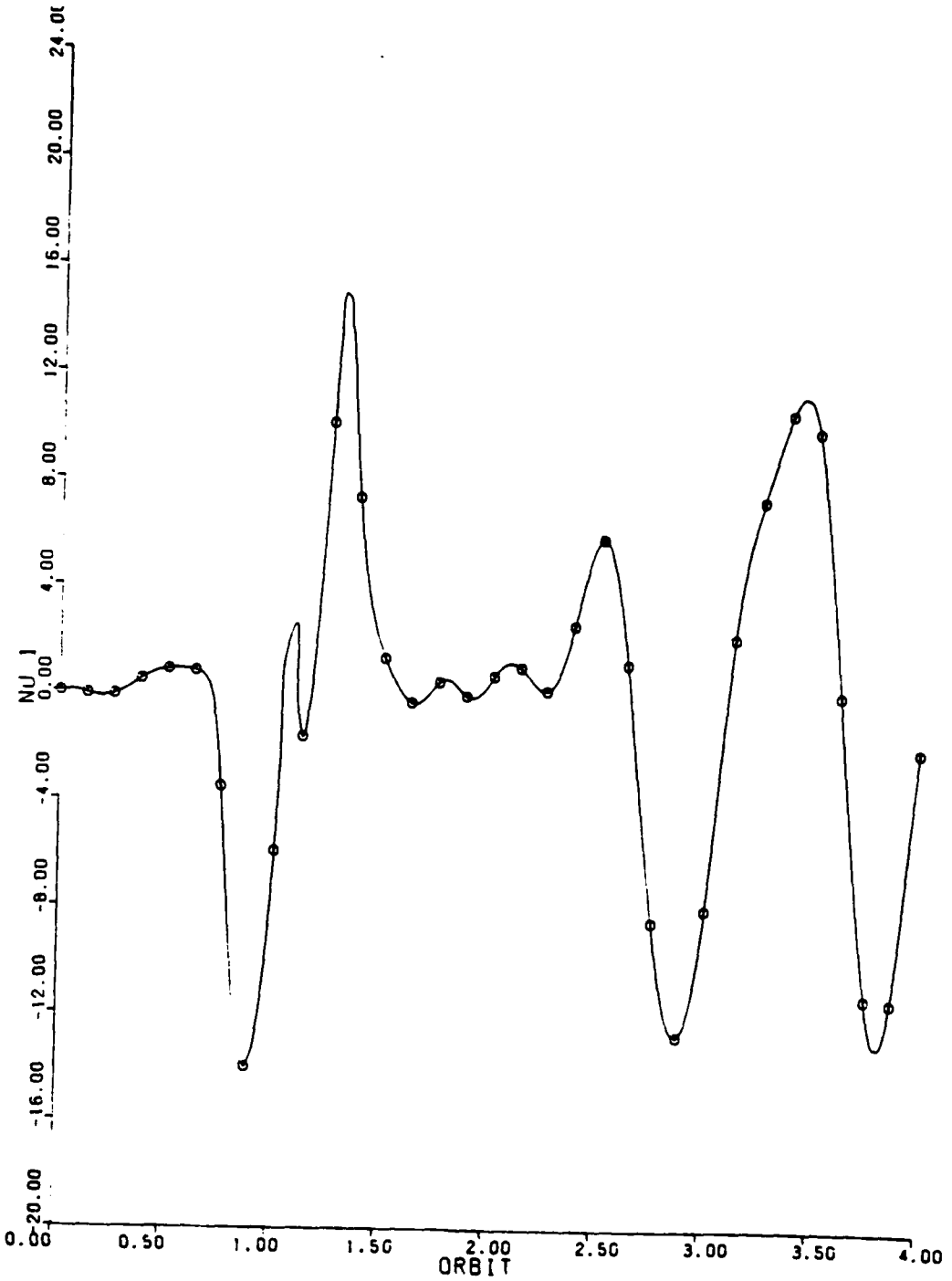

Figure 8: Modal Coordinate 1, With Eccentricity and Inclination, ($\bar{\delta x} \neq \bar{0}$, 4 Orbits)

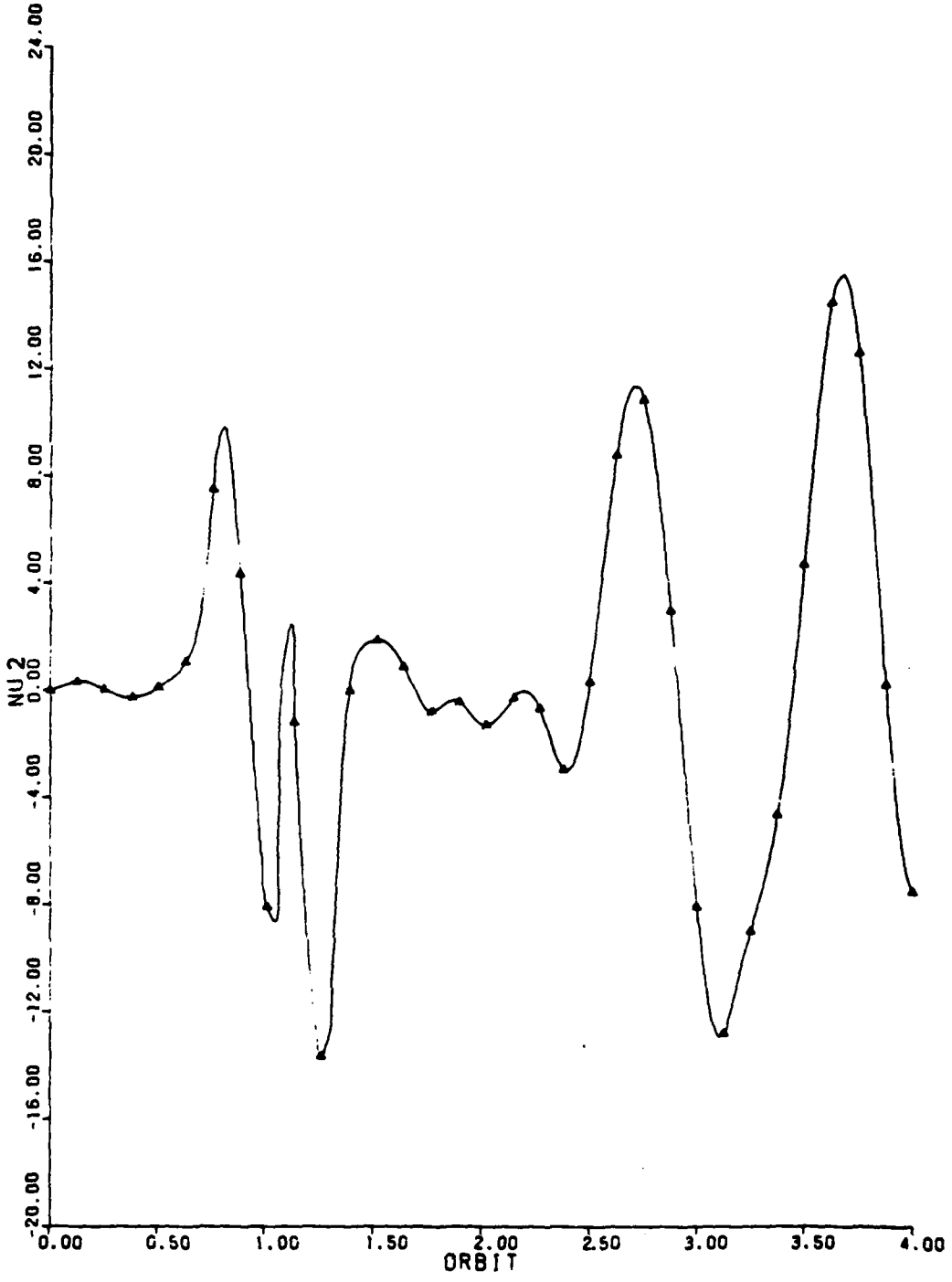

Figure 9: Modal Coordinate 2, With Eccentricity and Inclination, ($\bar{0}x\bar{+}\bar{0}$, 4 Orbits)

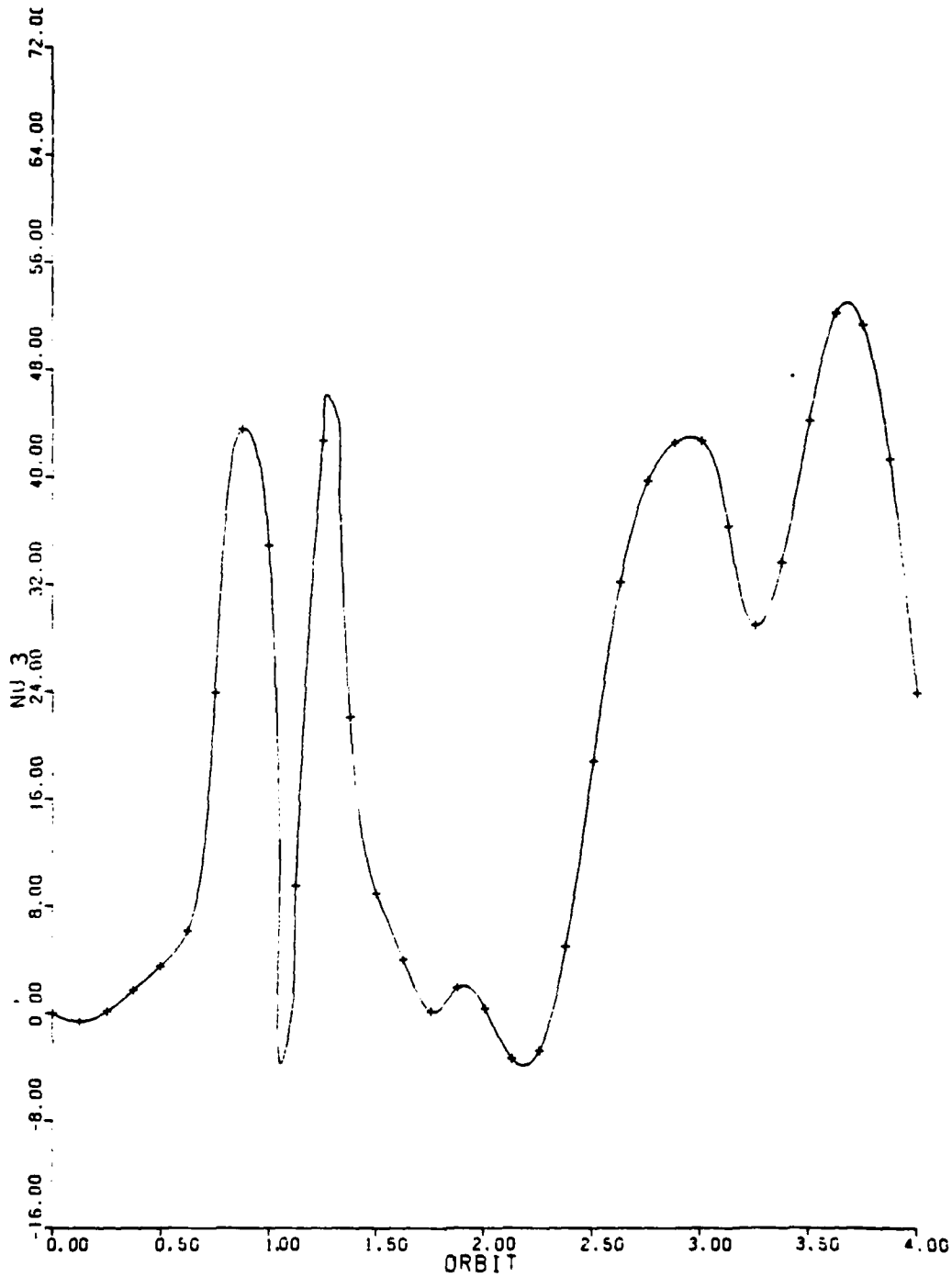

Figure 10: Modal Coordinate 3, With Eccentricity and Inclination,($\bar{\delta x} \neq \bar{0}$, 4 Orbits)

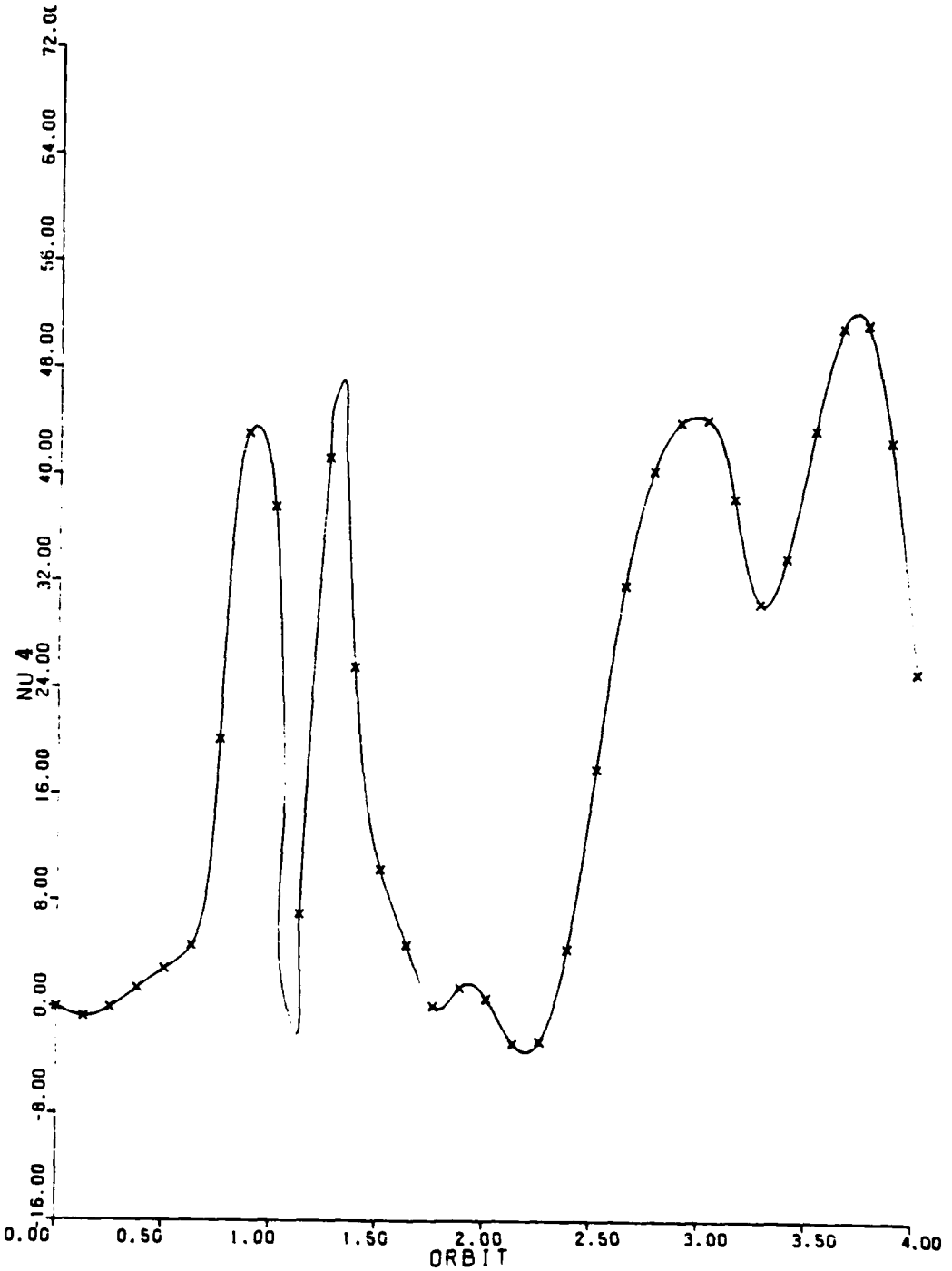

Figure 11: Modal Coordinate 4, With Eccentricity and Inclination,($\bar{\delta x} \neq \bar{0}$, 4 Orbits)

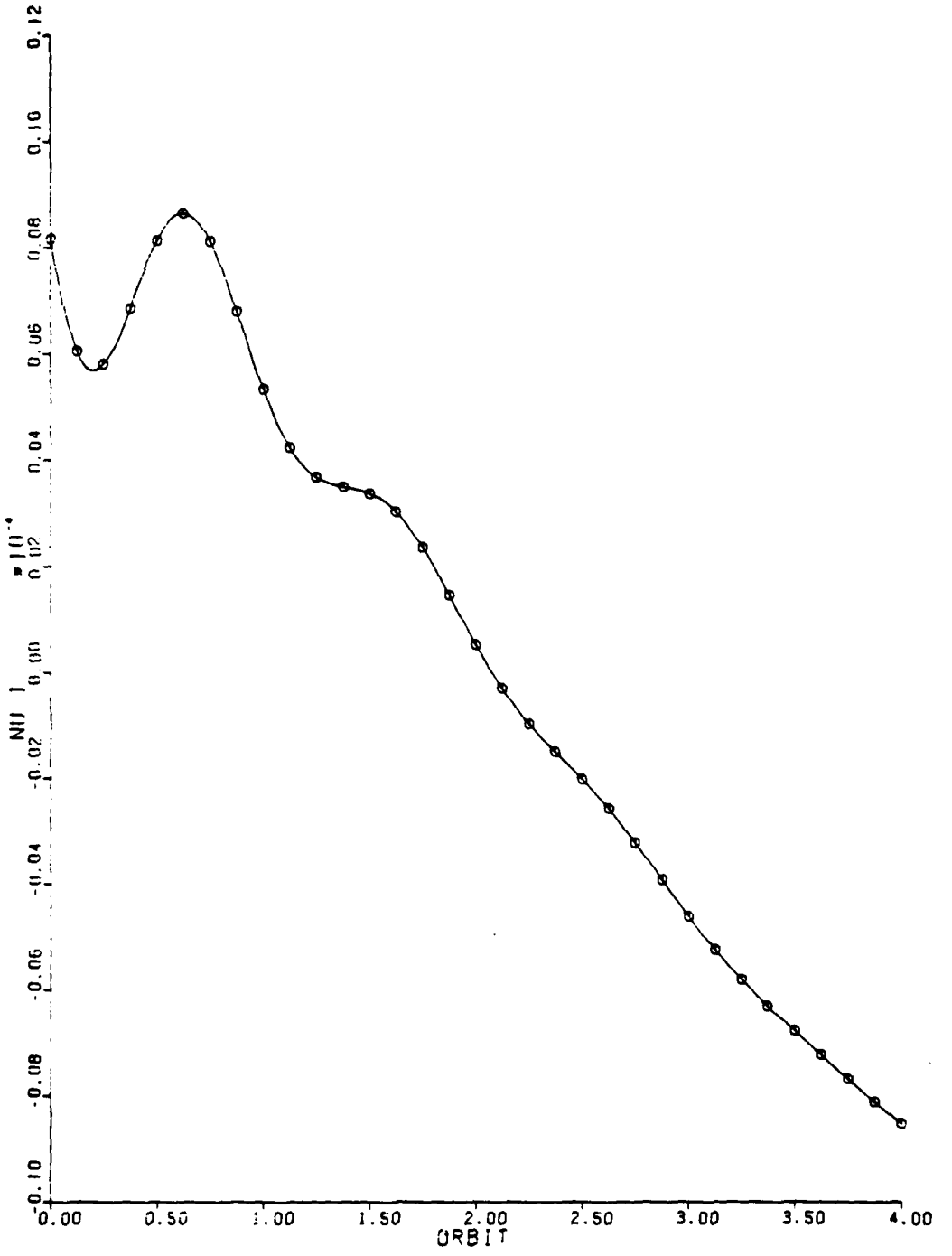

Figure 12: Modal Coordinate 1, Shelton Controller, ($\delta\bar{x} \neq \bar{0}$, 4 Orbits)

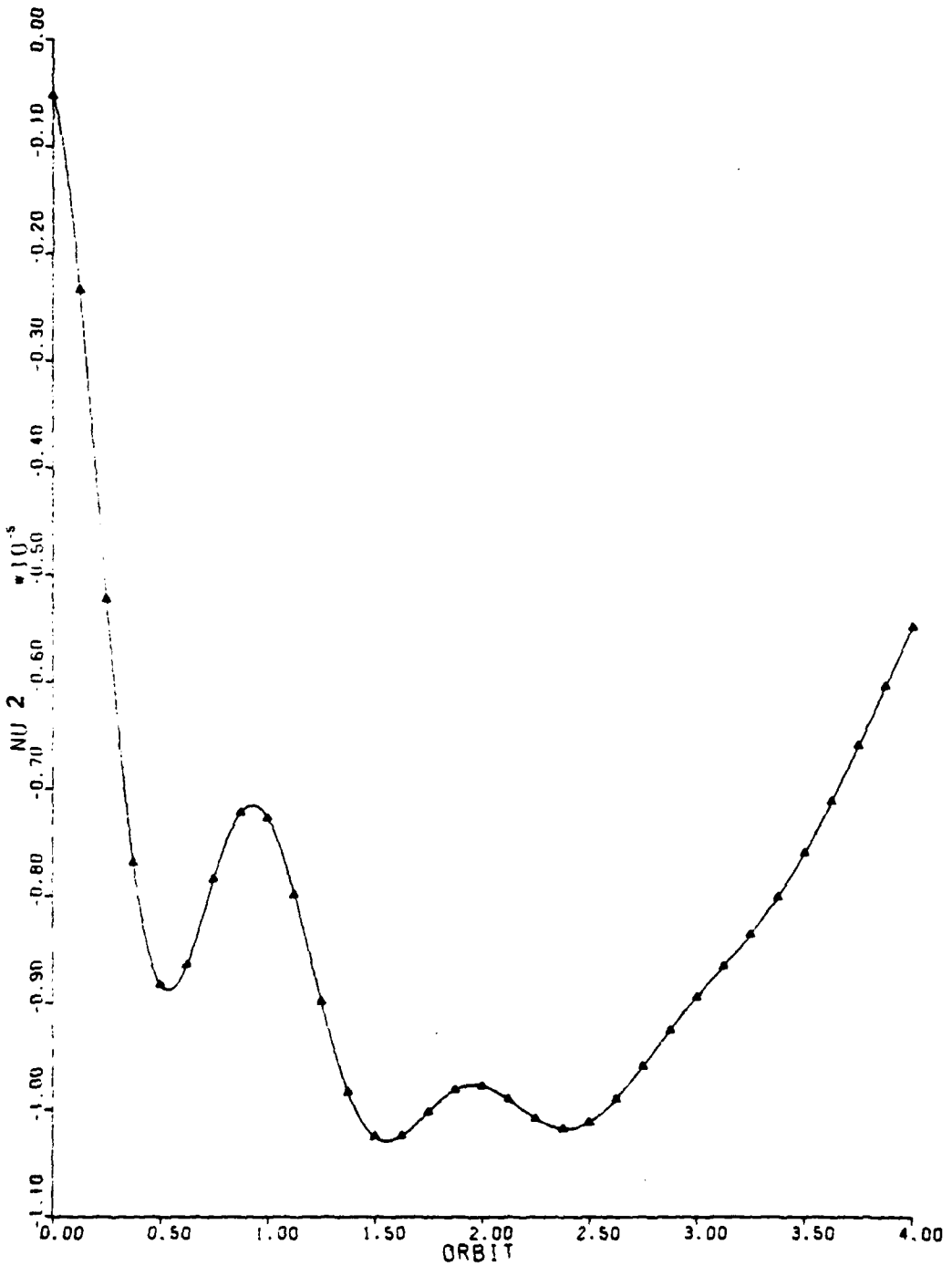

Figure 13: Modal Coordinate 2, Shelton Controller, ($\bar{\delta x} \neq \bar{0}$, 4 Orbits)

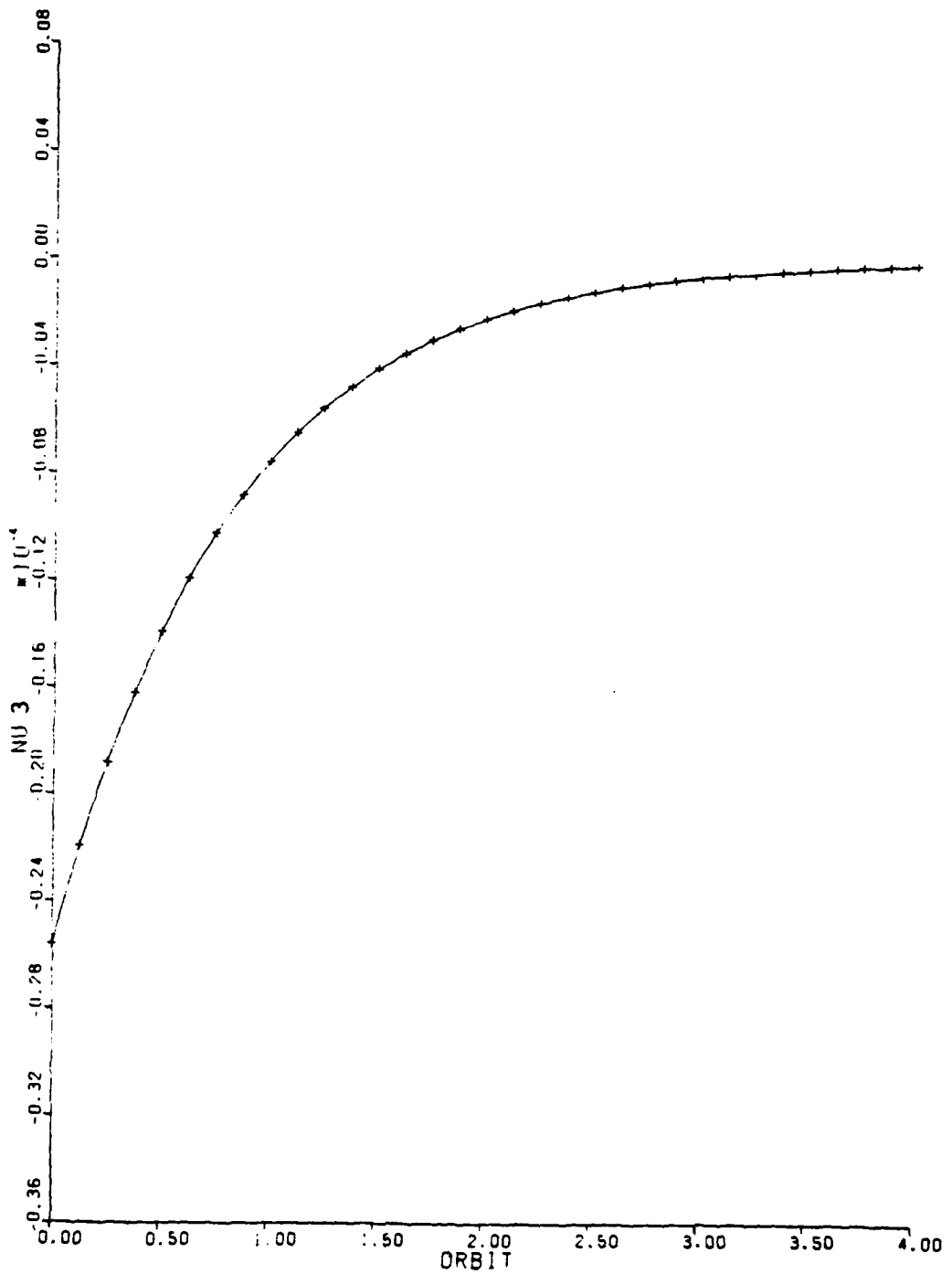

Figure 14: Modal Coordinate 3, Shelton Controller, ($\delta\bar{x} \neq \bar{0}$, 4 Orbits)

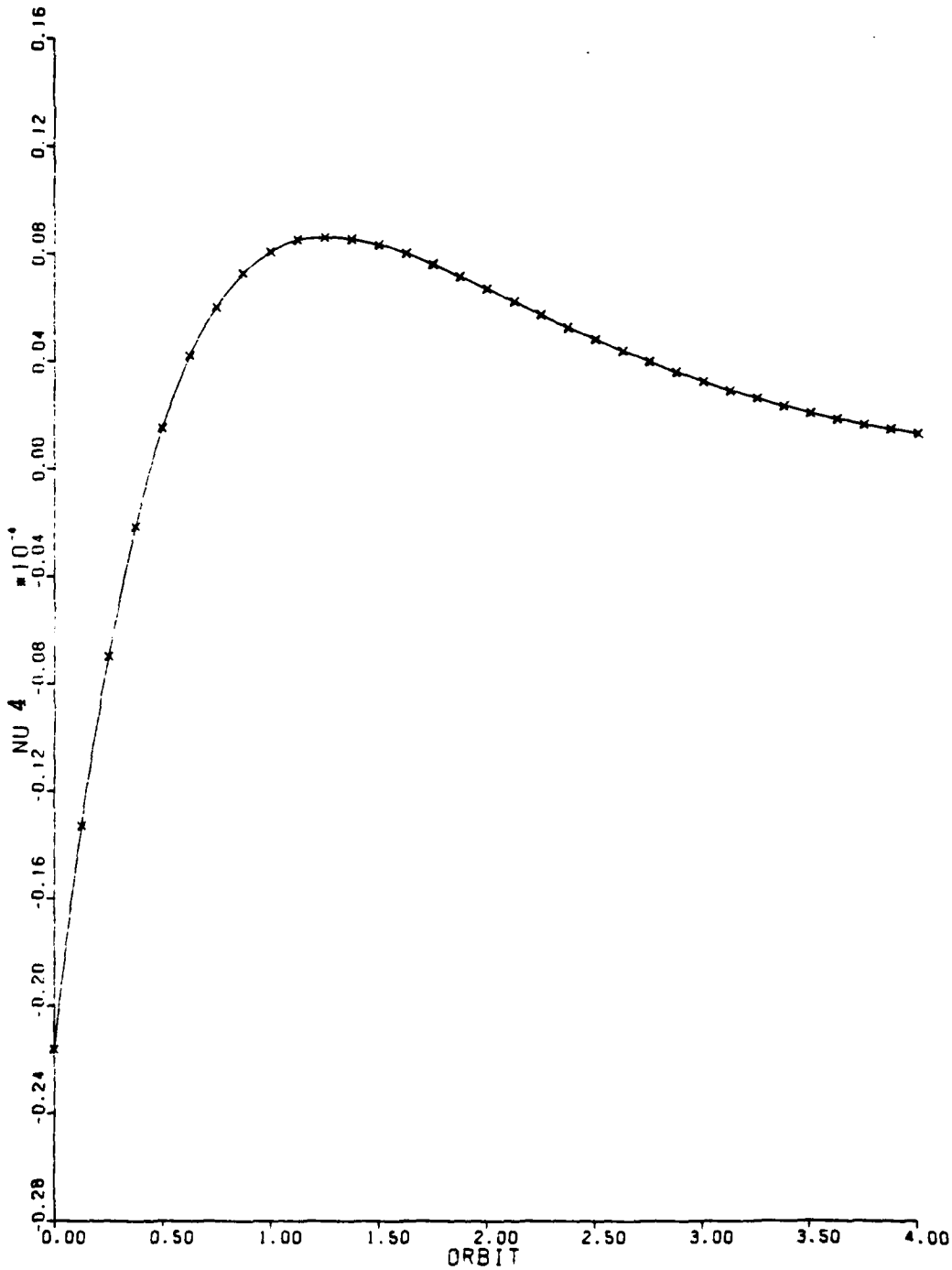

Figure 15: Modal Coordinate 4, Shelton Controller, ($\delta\bar{x} \neq \bar{0}$, 4 Orbits)

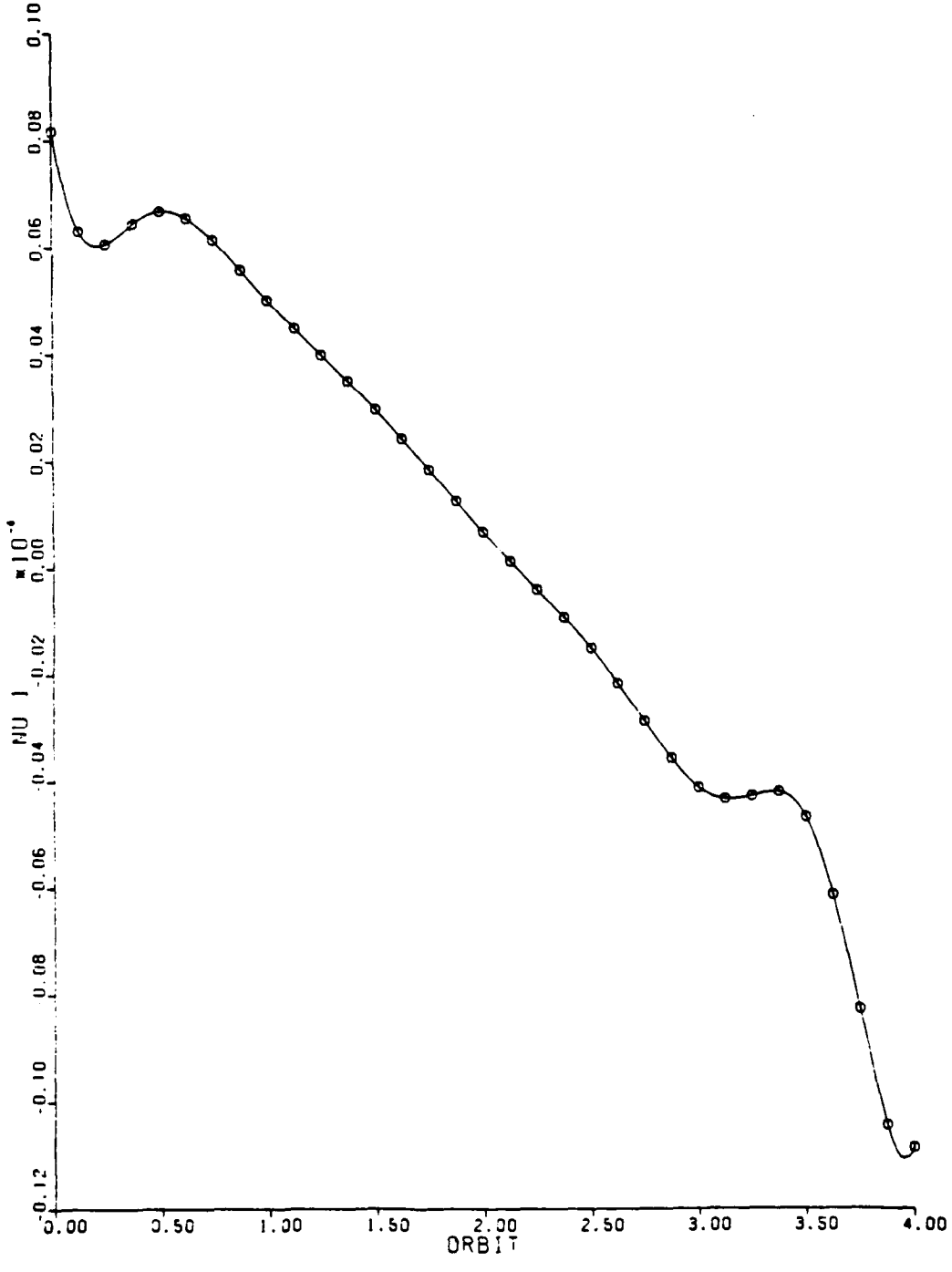

Figure 16: Modal Coordinate 1, DeArmond Controller, ($\bar{\delta x} \neq \bar{0}$, 4 Orbits)

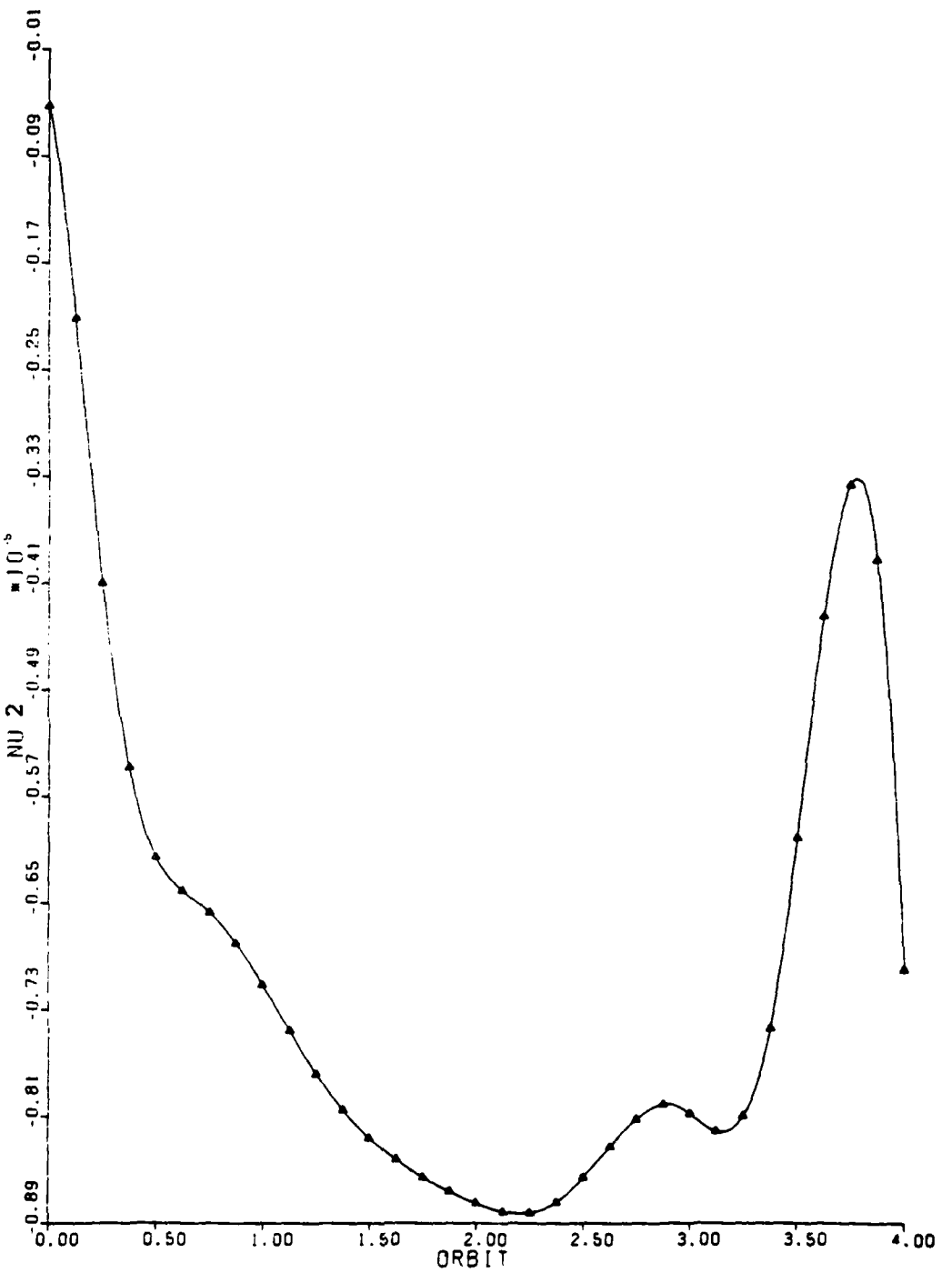

Figure 17: Modal Coordinate 2, DeArmond Controller, ($\bar{\delta x} \neq \bar{0}$, 4 Orbits)

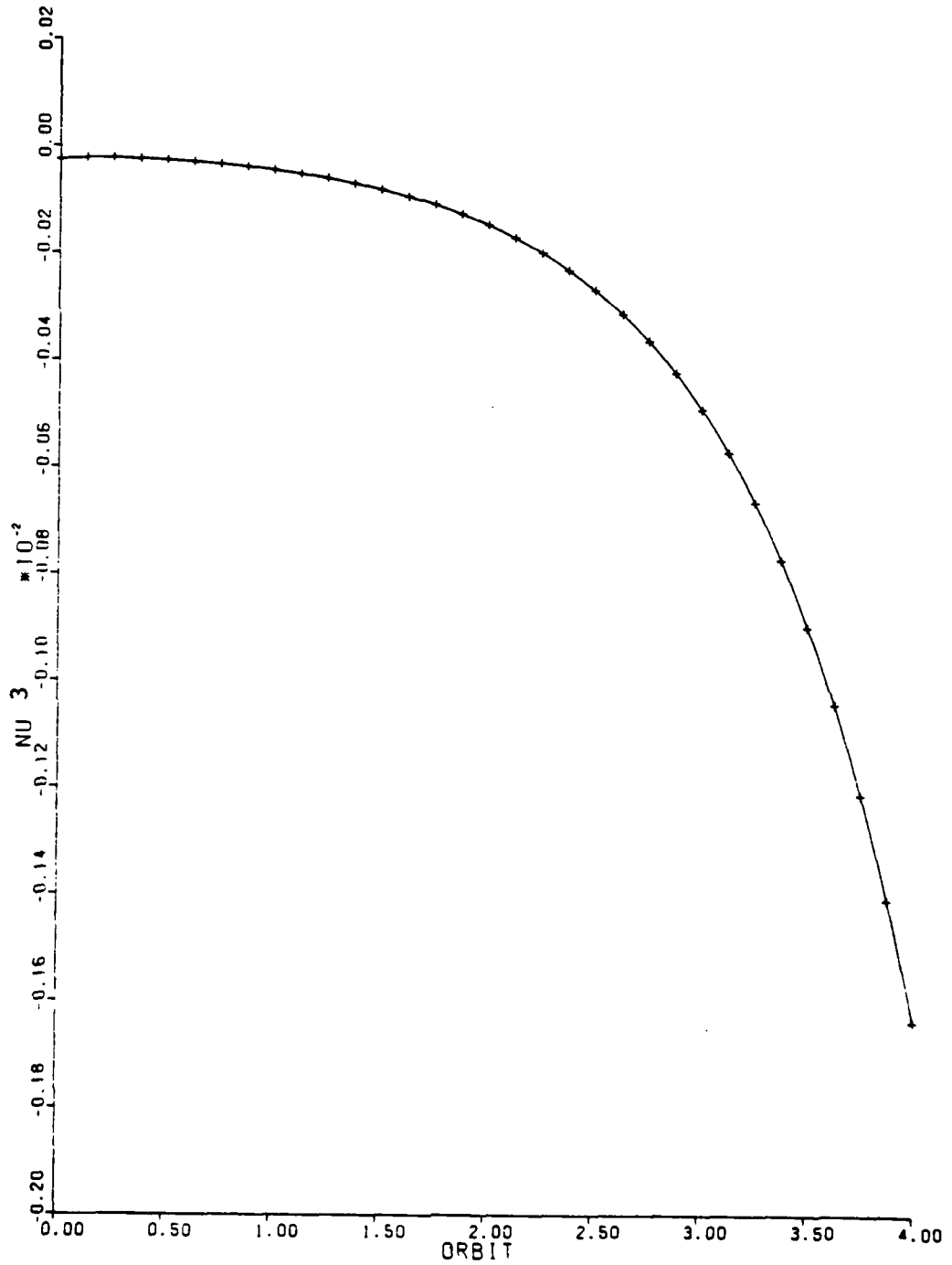

Figure 18: Modal Coordinate 3, DeArmond Controller, ($\delta\bar{x} \neq \bar{0}$, 4 Orbits)

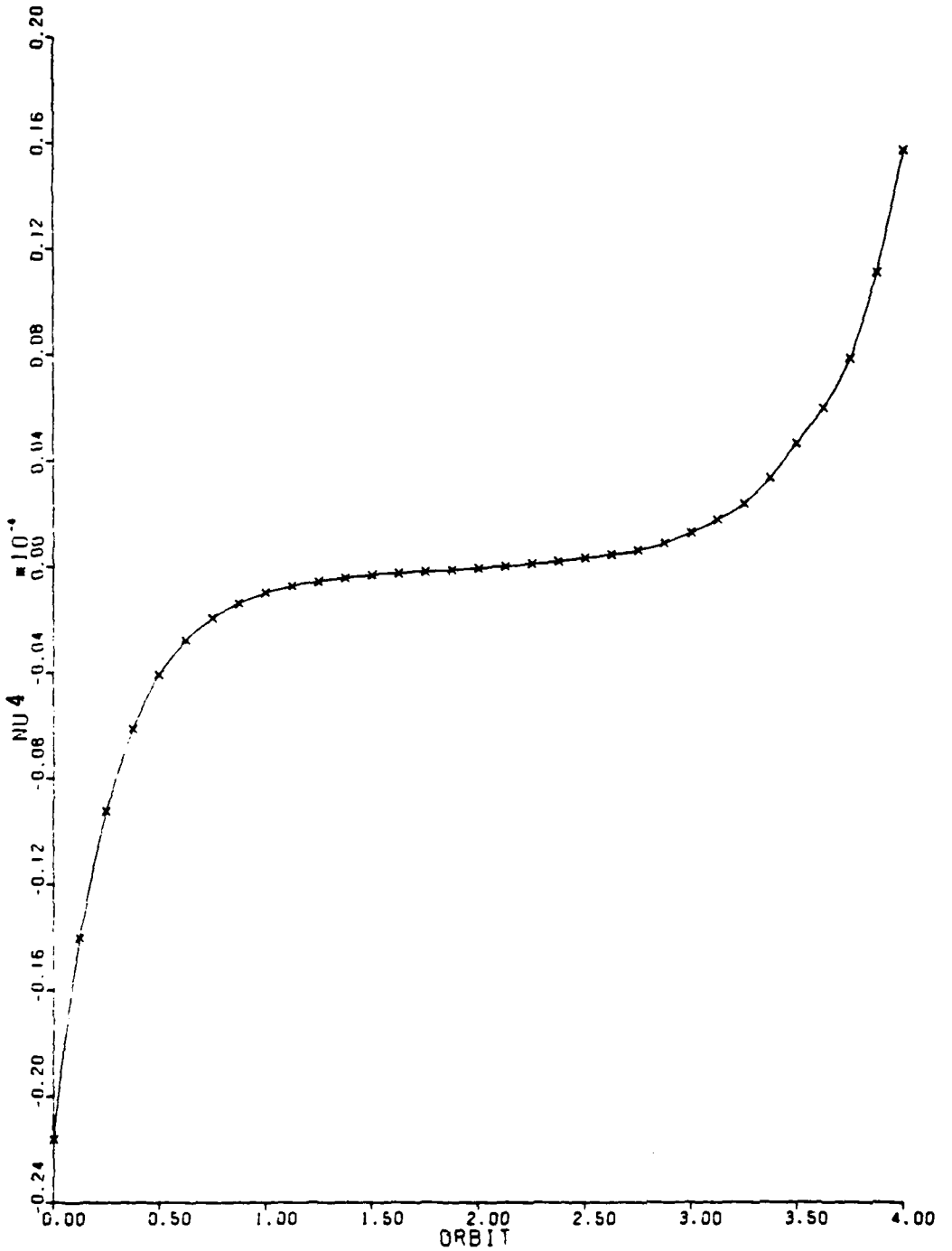

Figure 19: Modal Coordinate 4, DeArmond Controller, ($\bar{\delta x} \neq \bar{0}$, 4 Orbits)

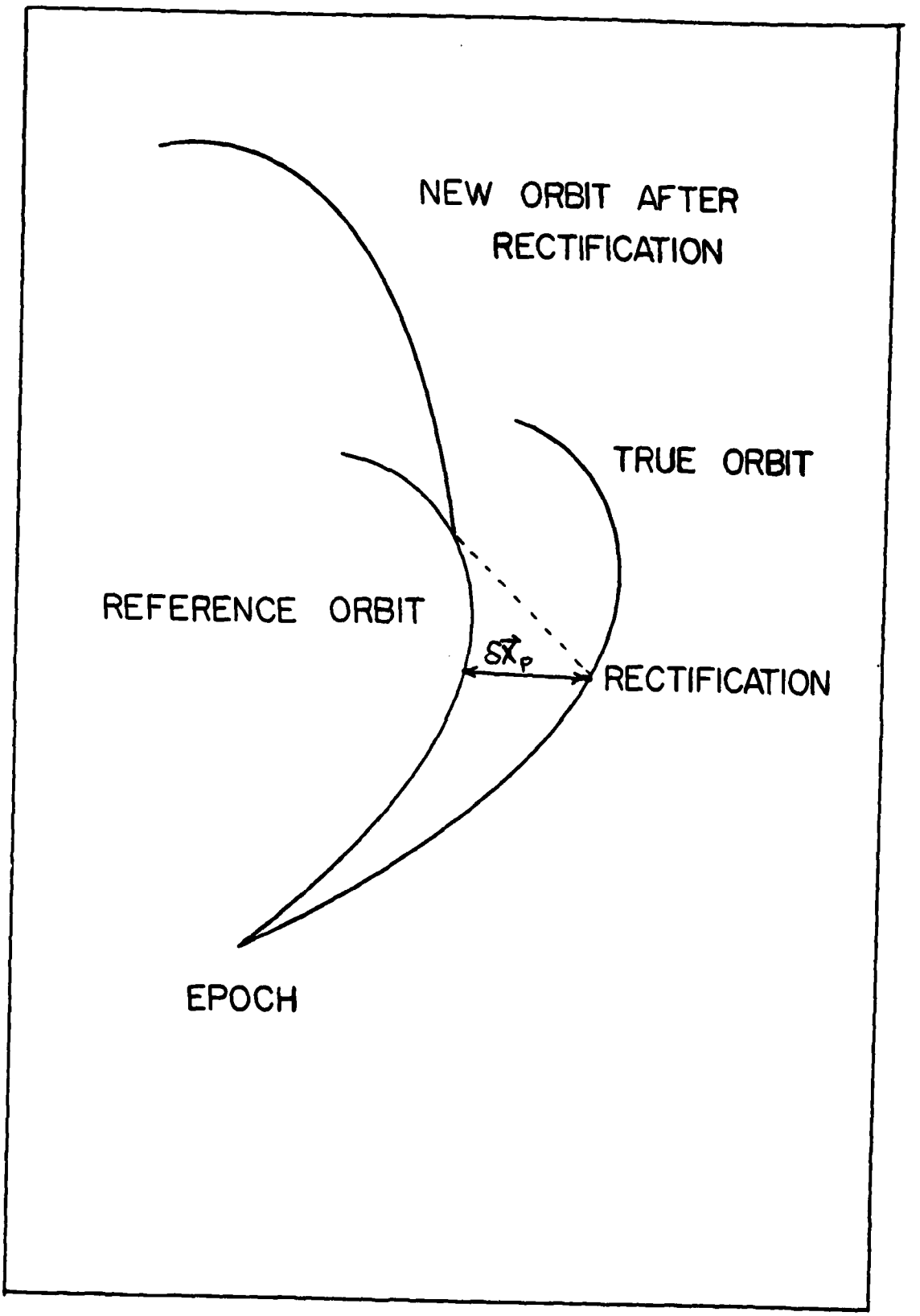

Figure 20: Reference Orbit With Rectification

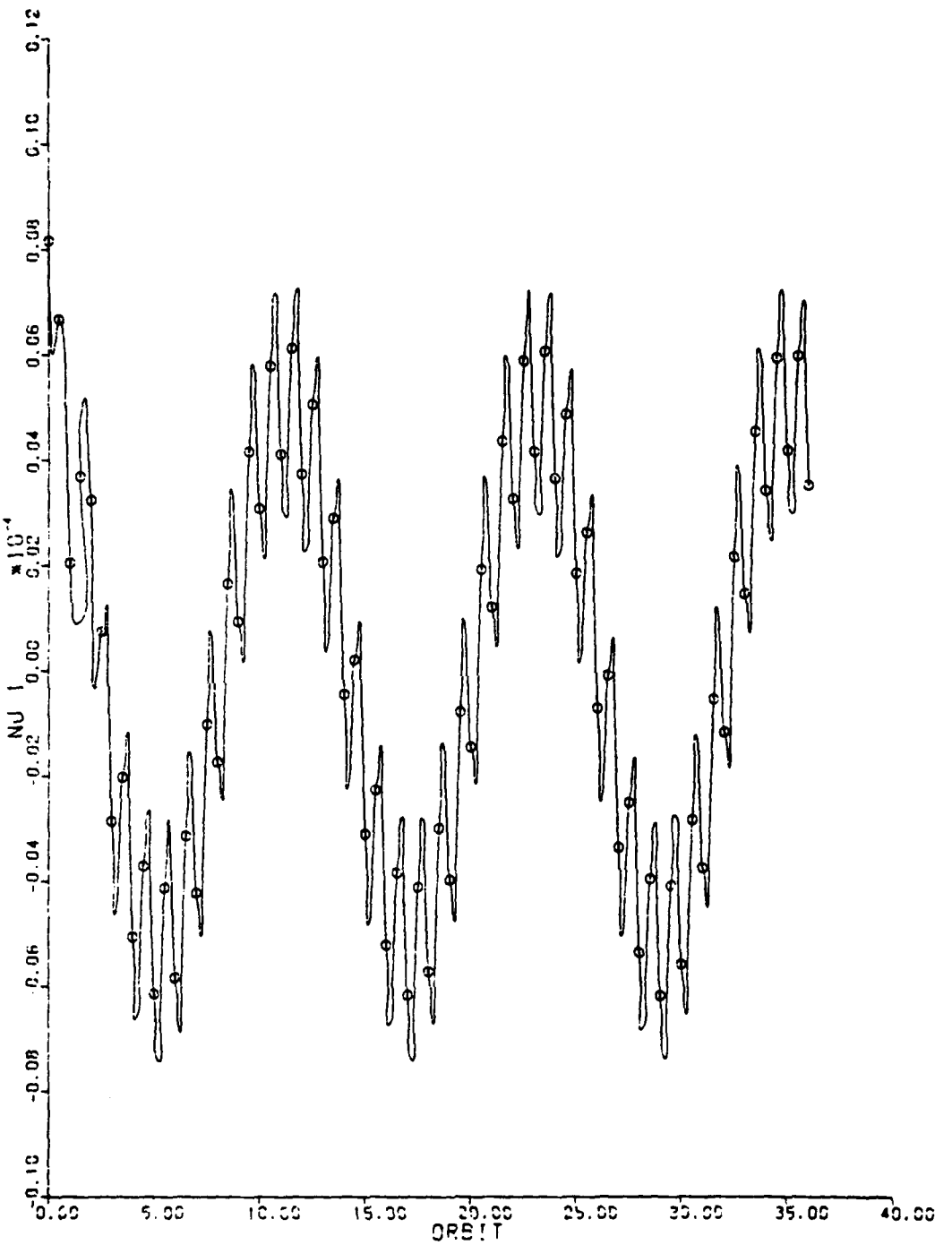

Figure 21: Modal Coordinate 1, Controller With Rectification, ($\delta\bar{x}(0) \neq \bar{0}$, 36 Orbits)

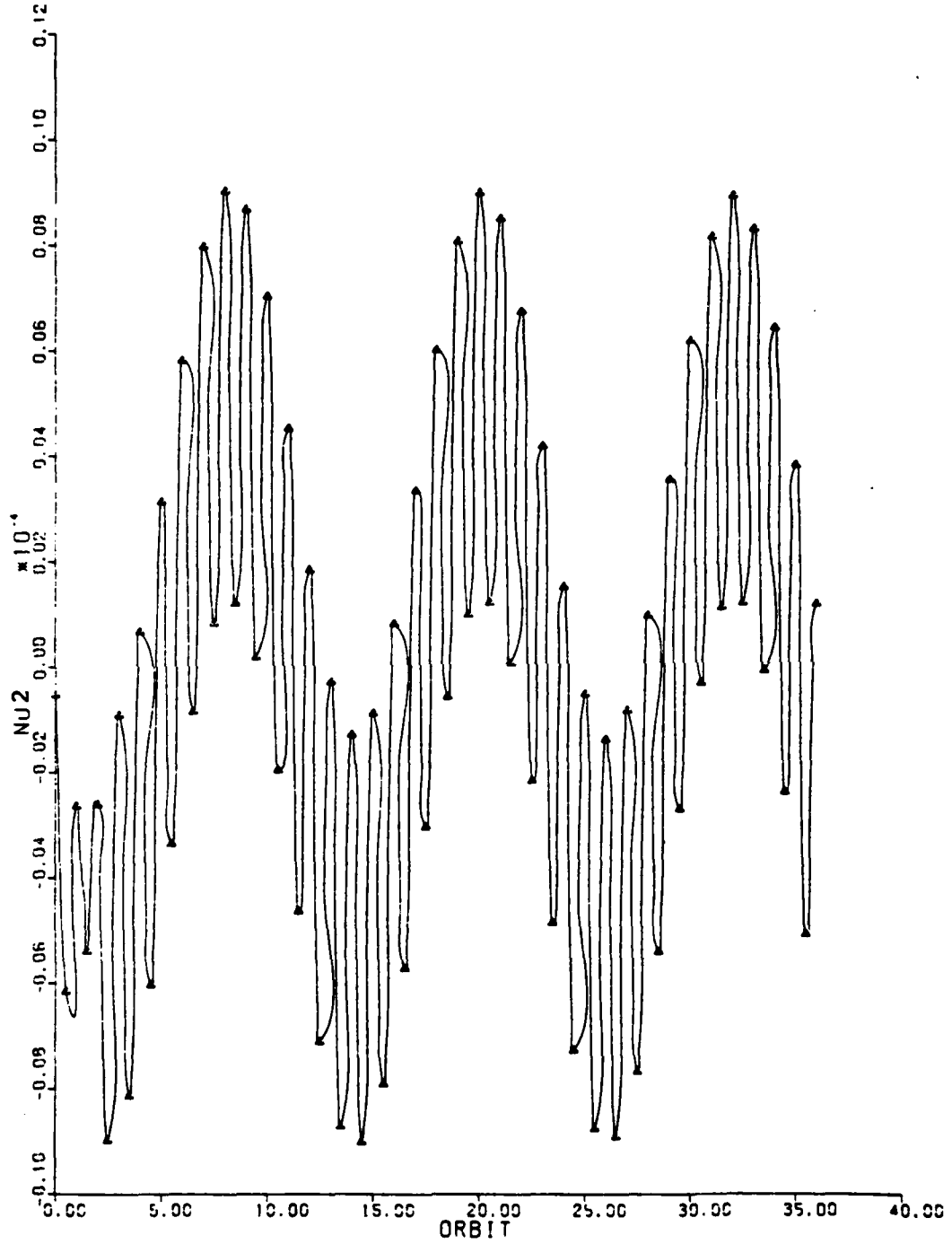

Figure 22: Modal Coordinate 2, Controller With Rectification, ($\delta\bar{x}(0) \neq \bar{0}$, 36 Orbits)

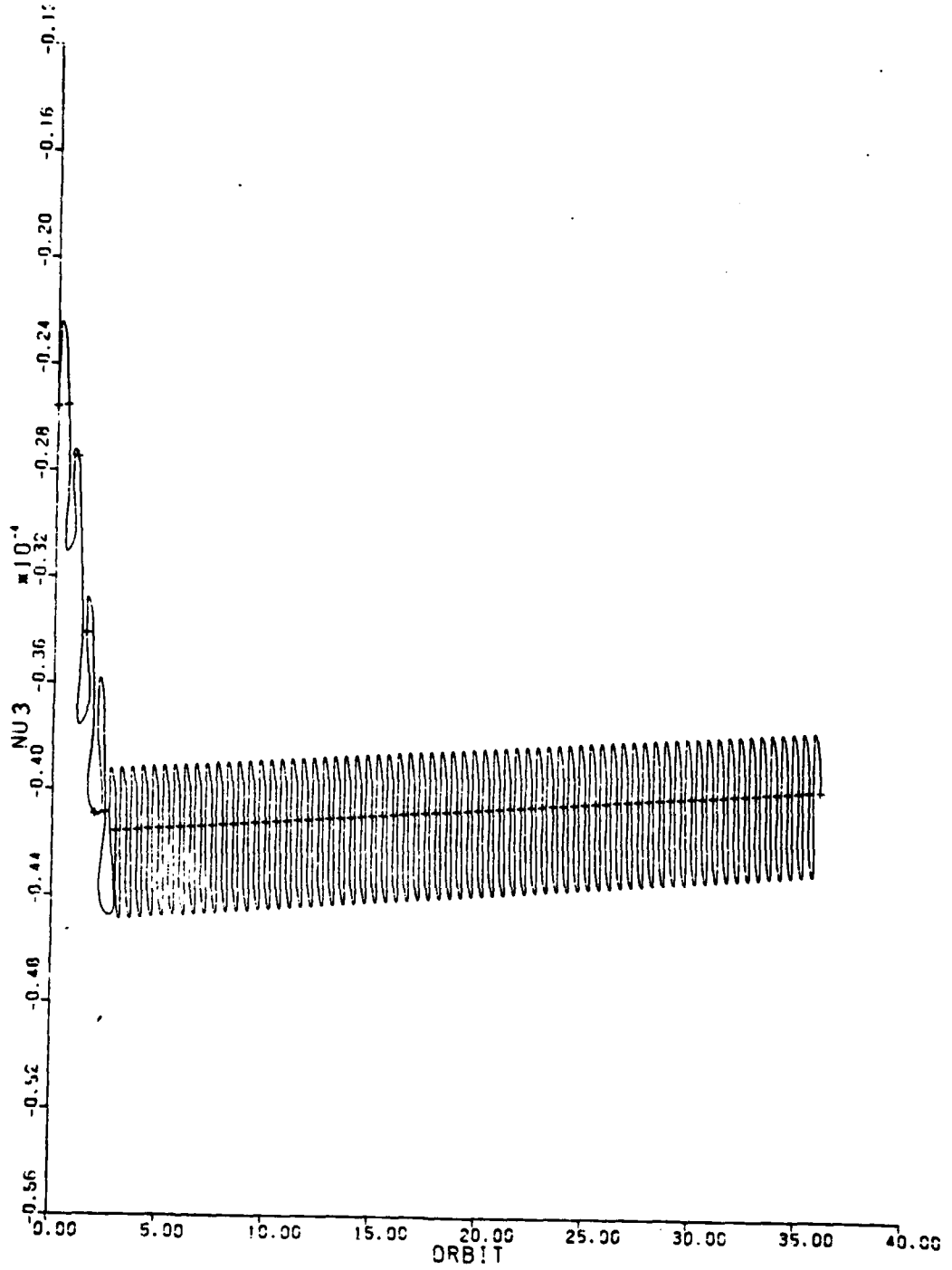

Figure 23: Modal Coordinate 3, Controller With Rectification, ($\bar{\delta x}(0) \neq \bar{0}$, 36 Orbits)

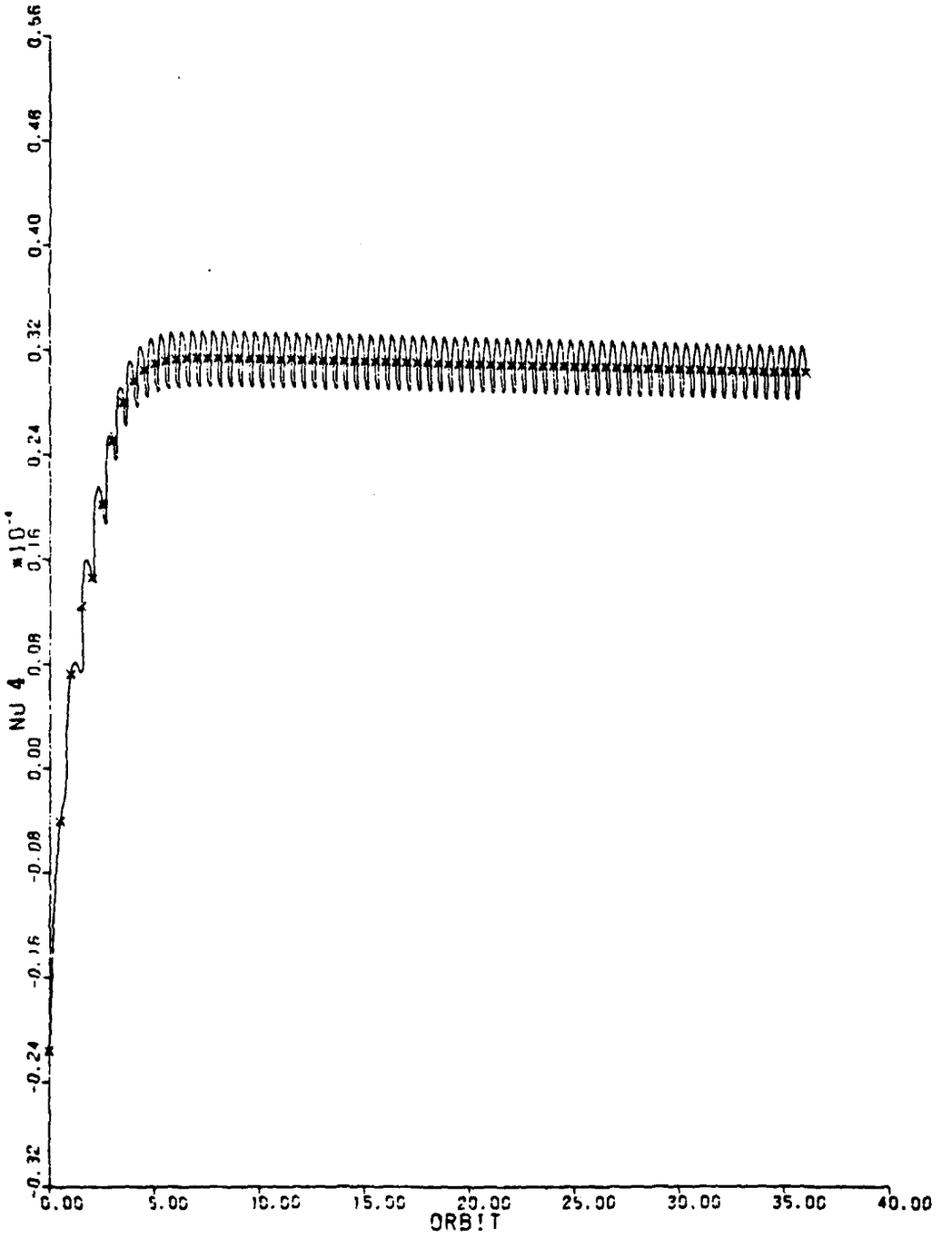

Figure 24: Modal Coordinate 4, Controller With Rectification, ($\bar{\delta x}(0) \neq \bar{0}$, 36 Orbits)

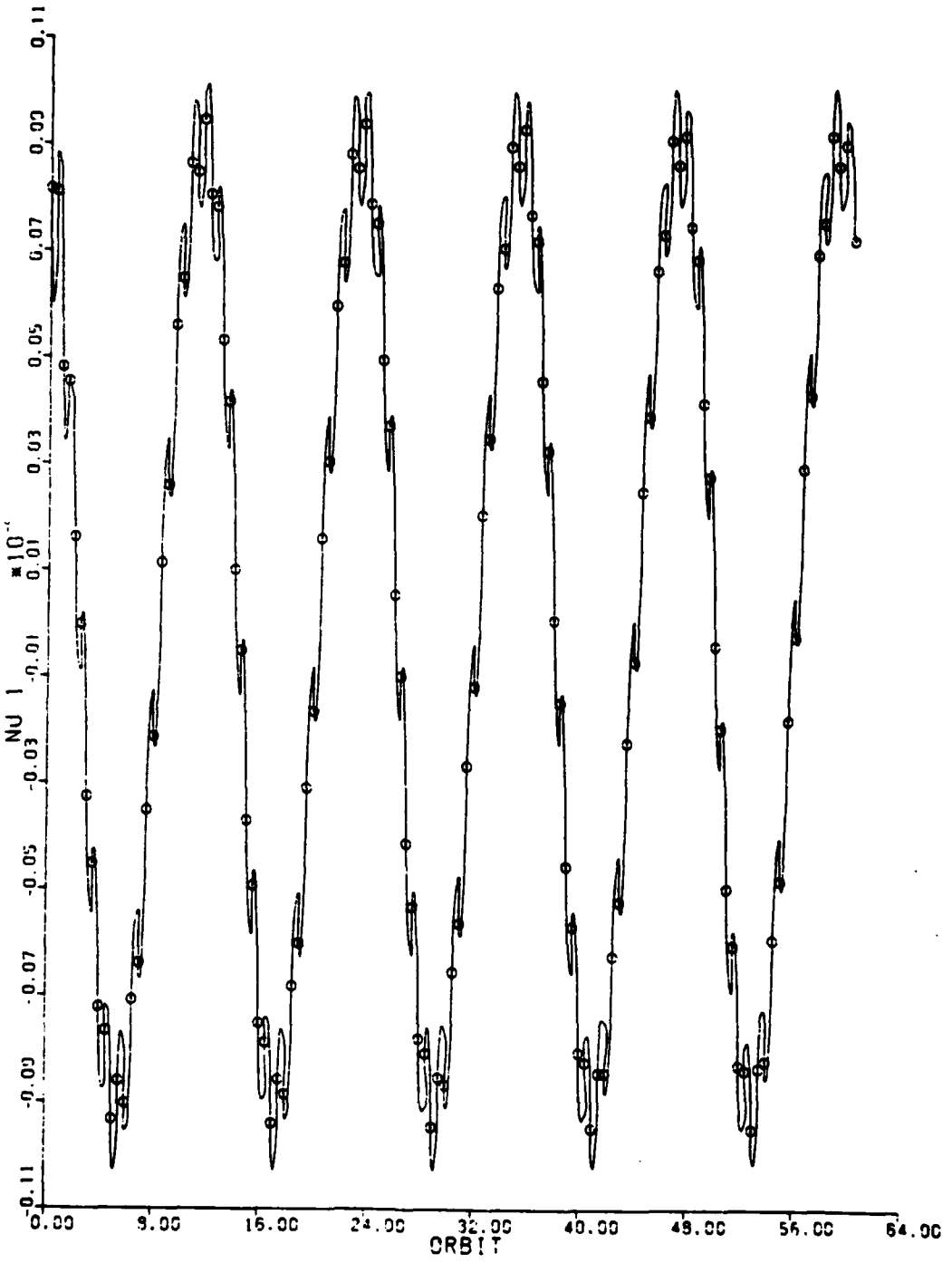

Figure 25: Modal Coordinate 1, Controller With Rectification, ($\delta\bar{x}+(\bar{0})$, 60 Orbits)

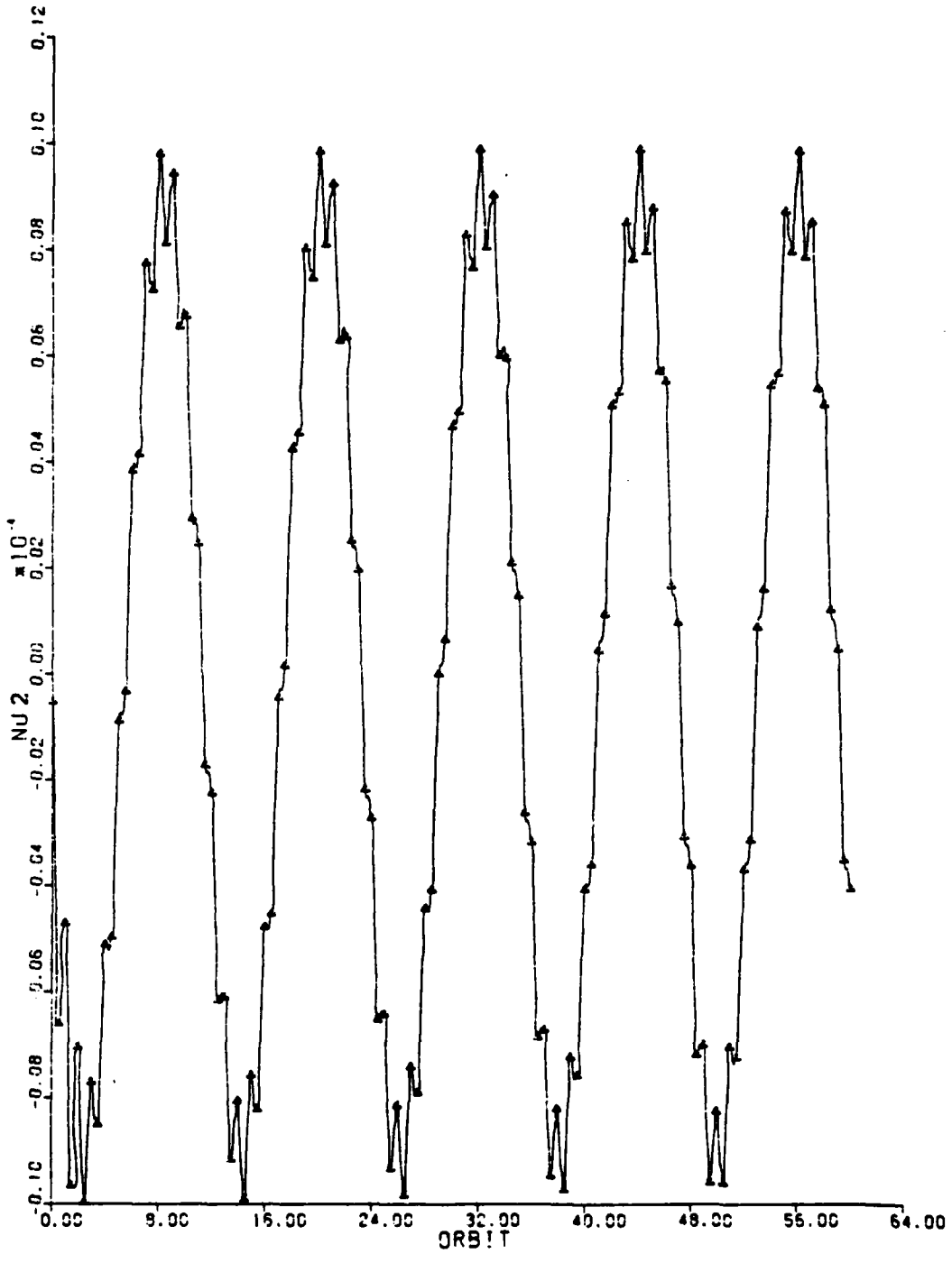

Figure 26: Modal Coordinate 2, Controller With Rectification, ($\overline{0x+}(\overline{0})$, 60 Orbits)

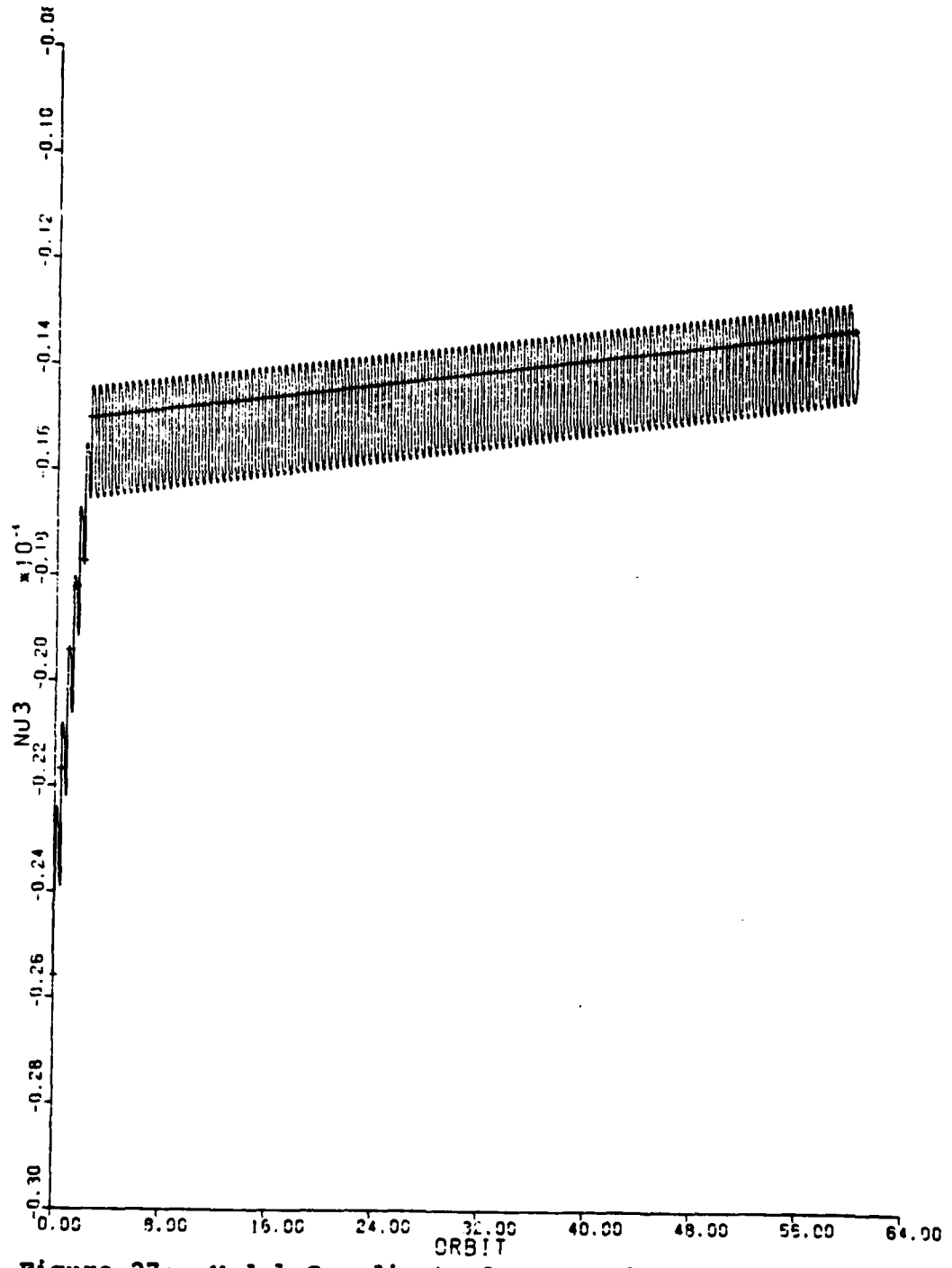

Figure 27: Modal Coordinate 3, Controller With Rectification, ($\delta\bar{x}+(\bar{0})$, 60 Orbits)

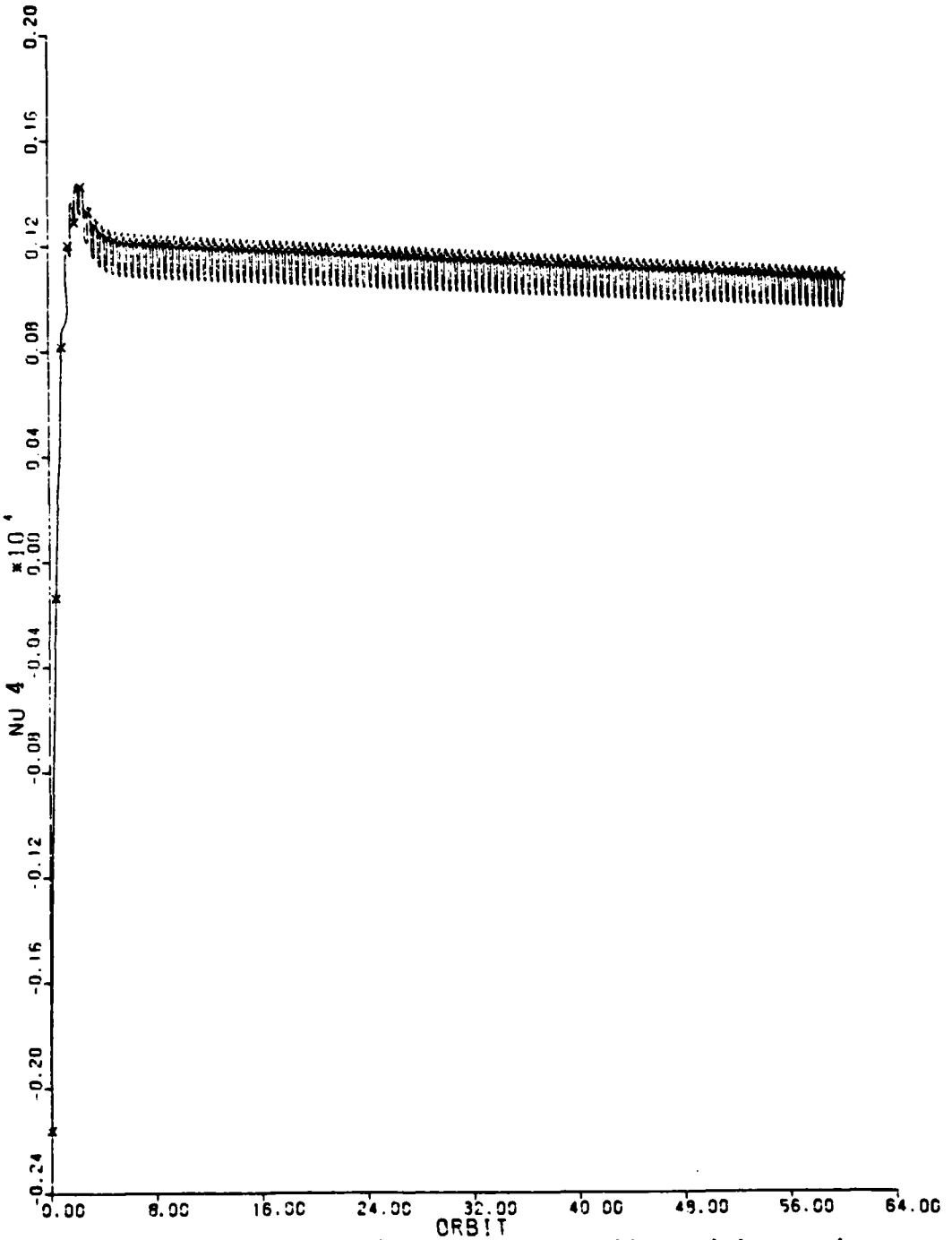

Figure 28: Modal Coordinate 4, Controller With Rectification, ($\delta\bar{x}+(\bar{0})$, 60 Orbits)

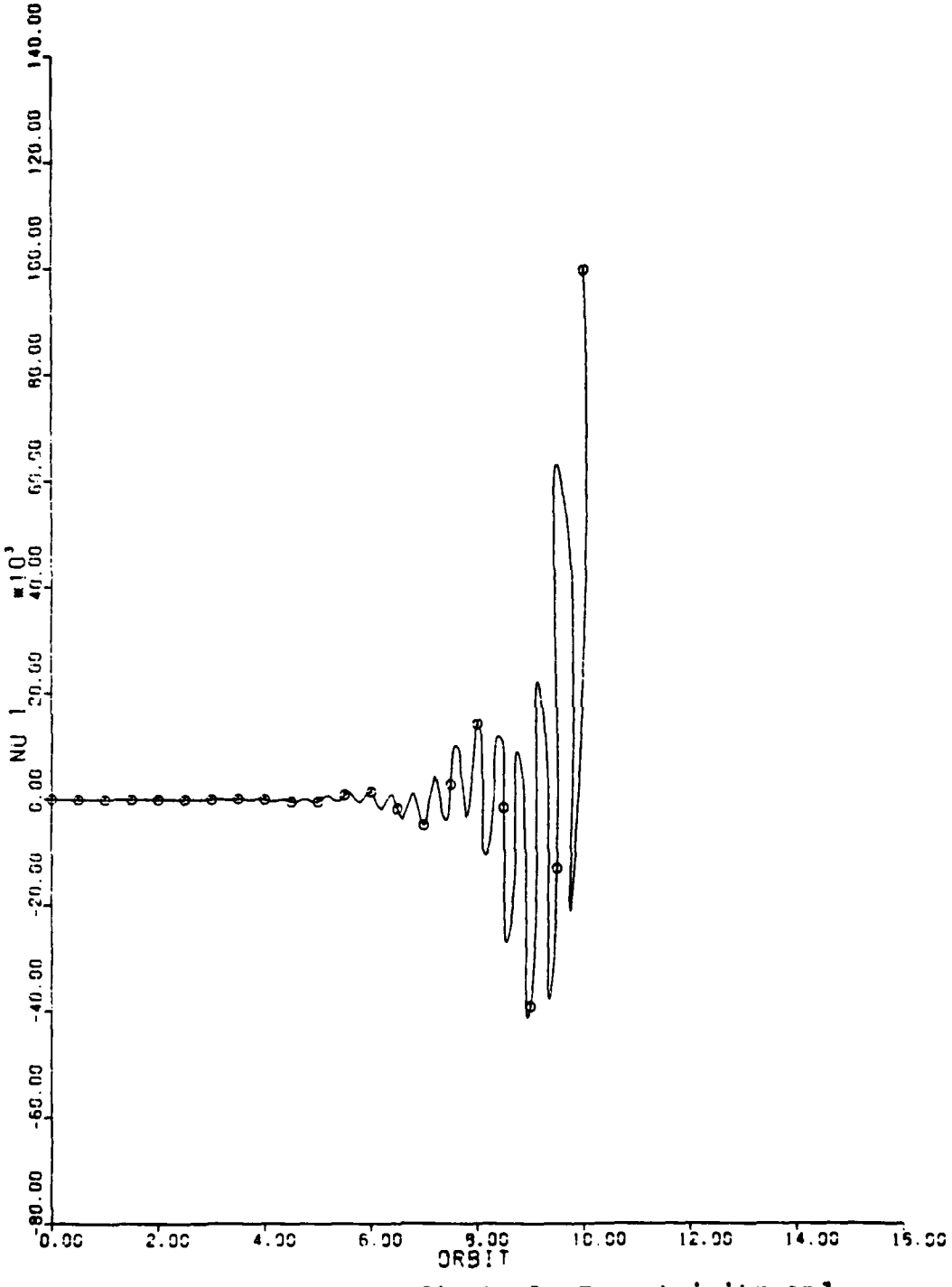

Figure 29: Modal Coordinate 1, Eccentricity and Inclination Included

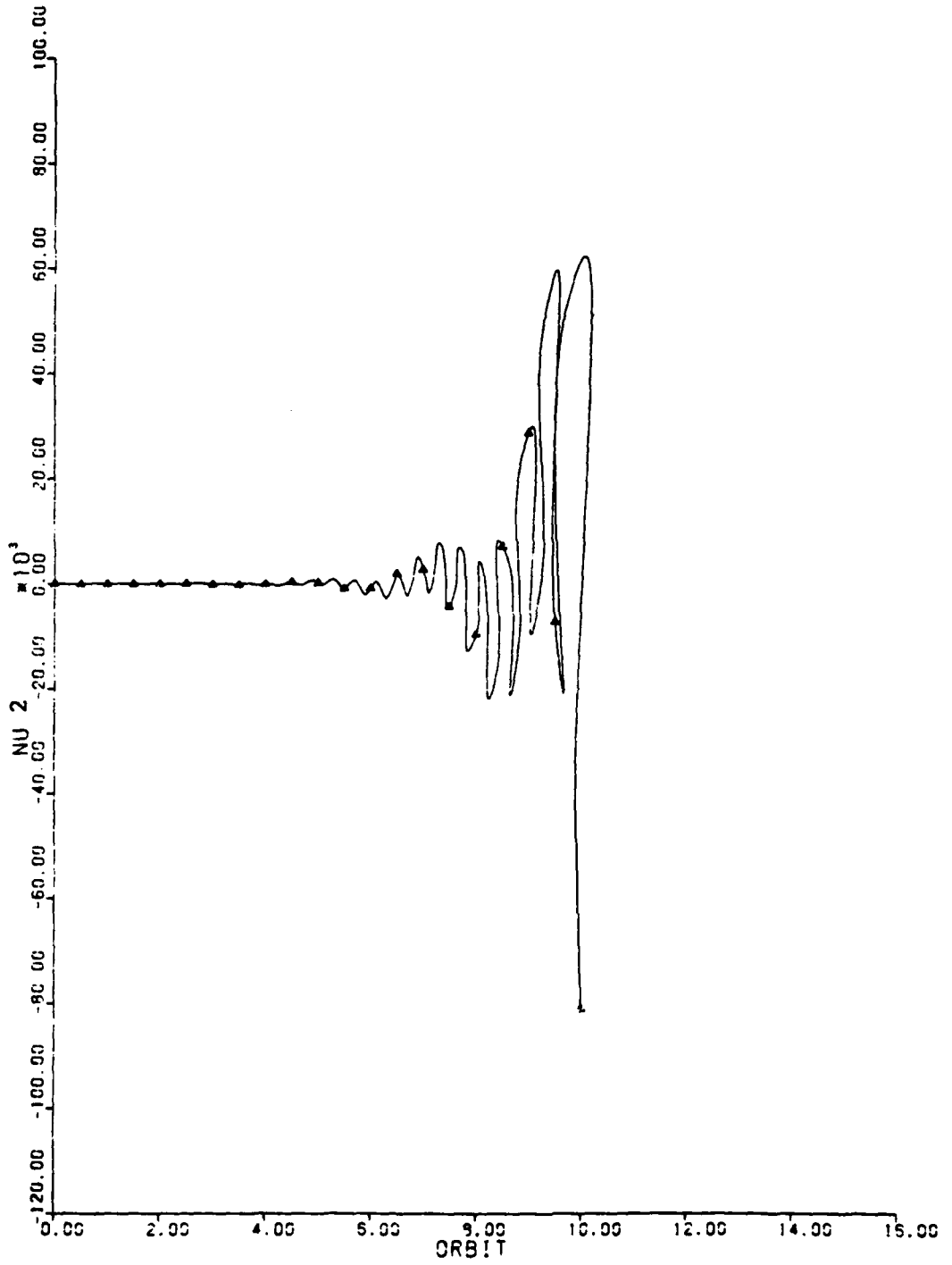

Figure 30: Modal Coordinate 2, Eccentricity and Inclination Included

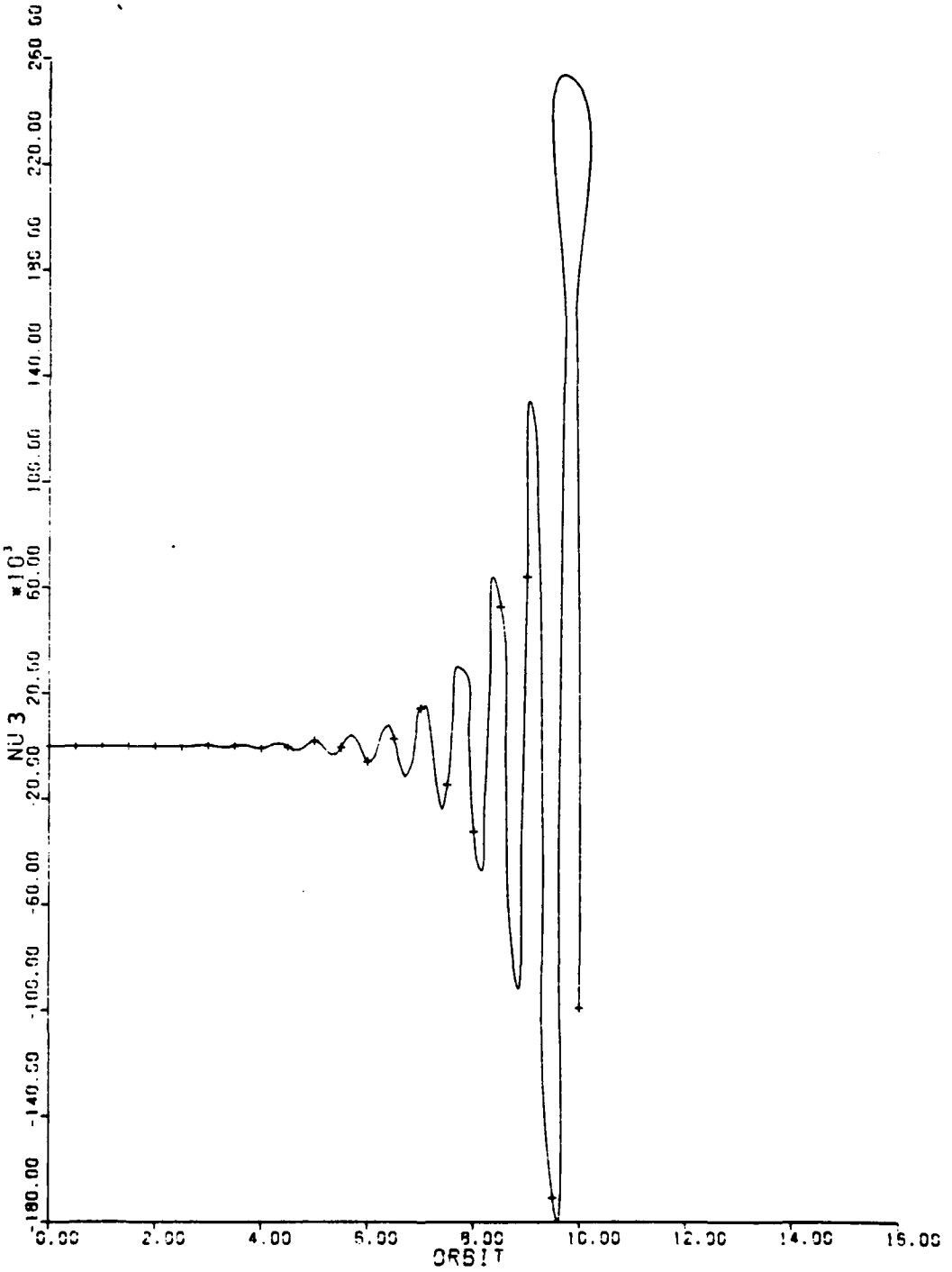

Figure 31: Modal Coordinate 3, Eccentricity and Inclination Included

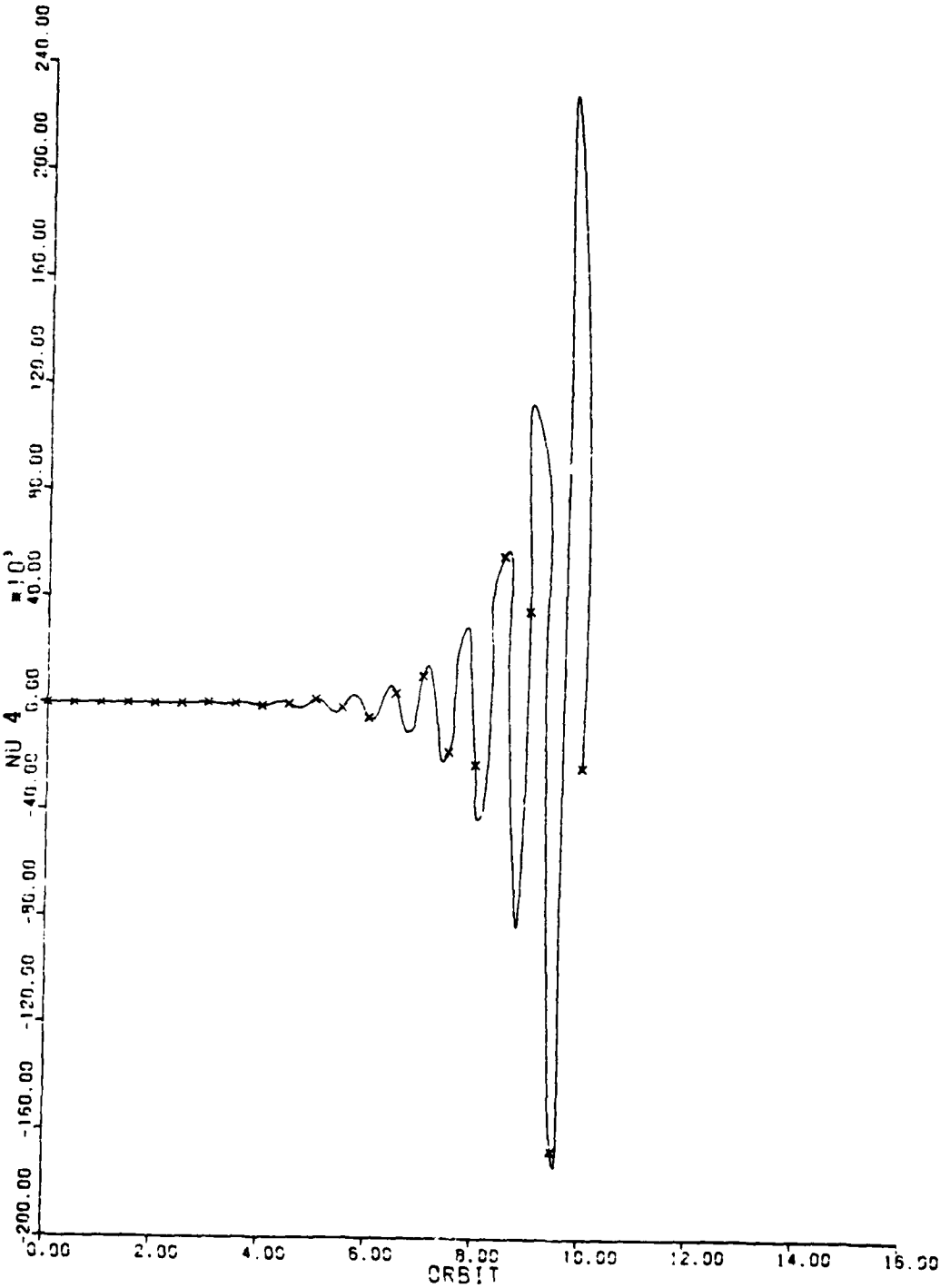

Figure 32: Modal Coordinate 4, Eccentricity and Inclination Included

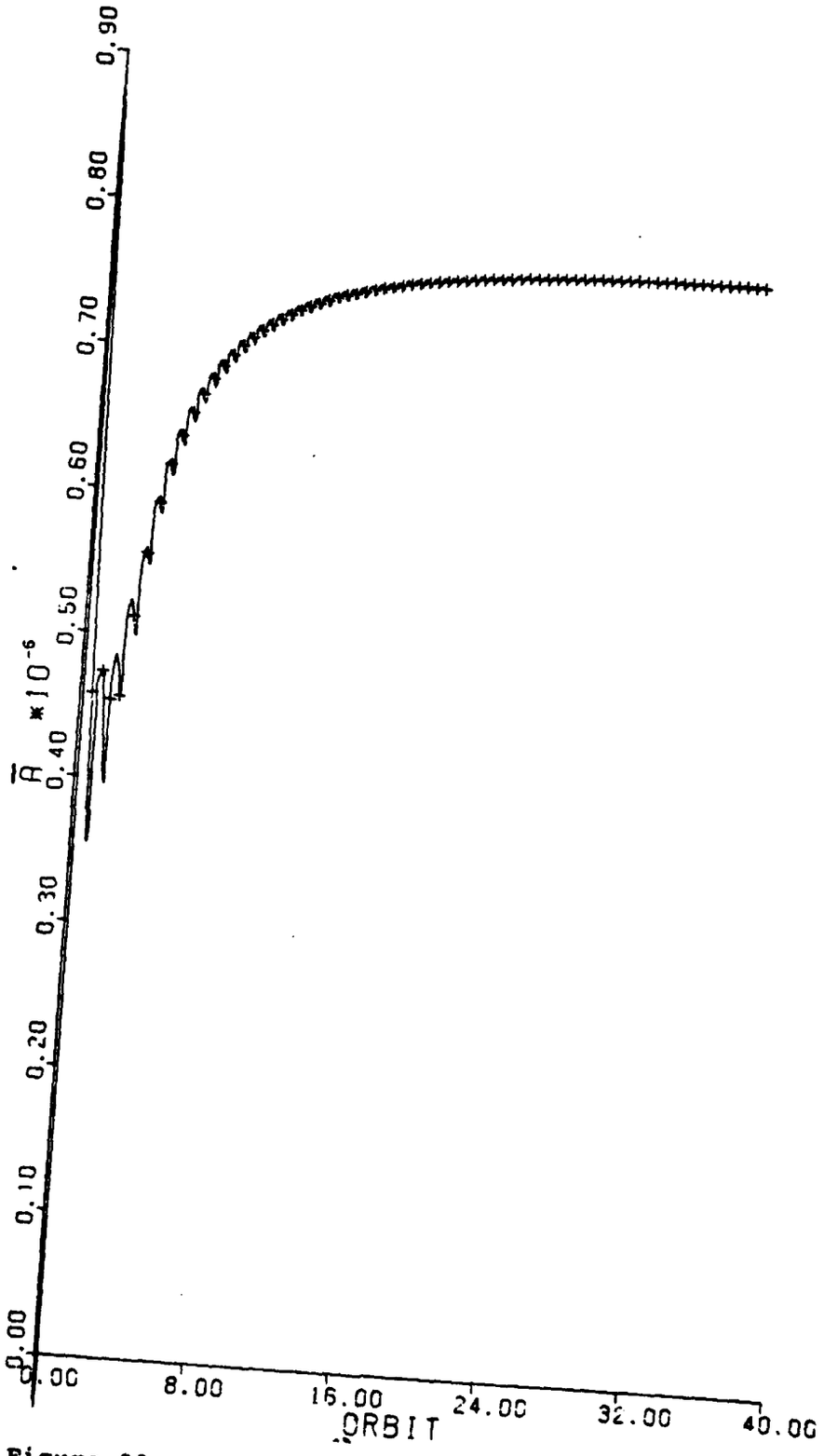

Figure 33: Average Acceleration $\bar{A}$, Versus Orbits, ($\delta x_{p_{avg}}$ max = 1. x 10^{45})

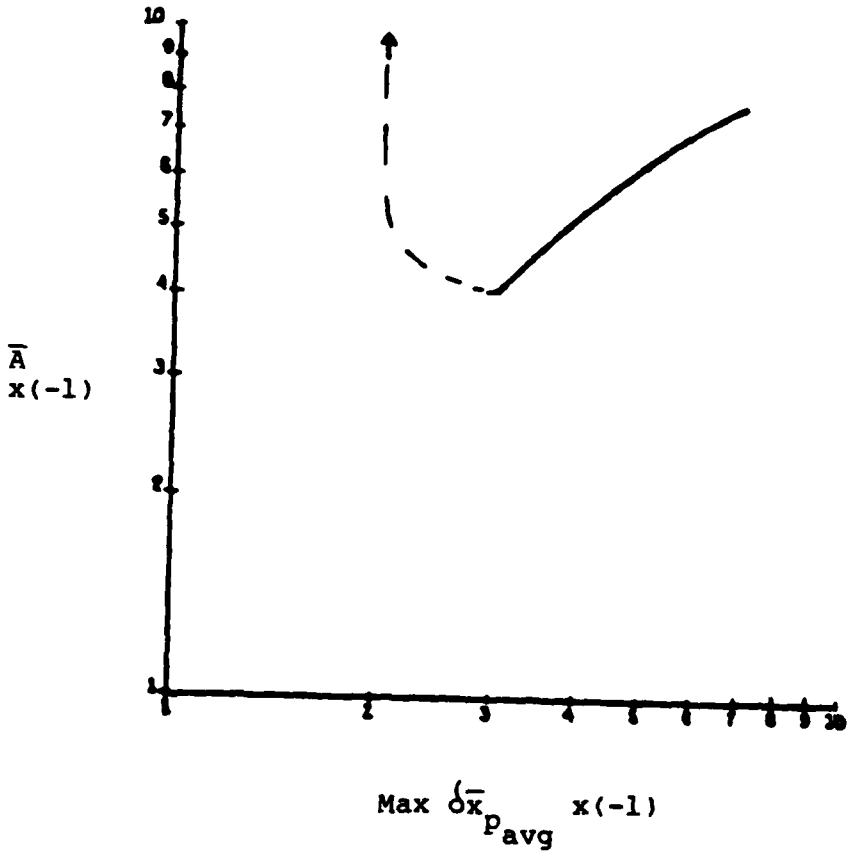

Figure 34: Average Acceleration, $\bar{A}$, Versus $\delta\bar{x}_{p_{avg_{max}}}$

Vita

Frank M. DeArmond was born 22 November 1954, at Fort Jackson, Columbia, S.C. In 1960, he and his family moved to Charlotte, N.C. where he attended Grammer, Junior High and High School. In August, 1973, he entered Embry-Riddle Aeronautical University. In August, 1976, DeArmond entered N.C. State University and graduated in 1978 with a Bachelor of Science Degree in Aerospace Engineering.

In June, 1978, DeArmond was assigned to the 6595th Shuttle Test group at Vandenberg AFB, CA, and there spent three years assisting in the development of the Space Shuttle Program at the Western Test Range.

In May, 1981, DeArmond was reassigned to the Air Force Institute of Technology at Wright-Patterson AFB, Ohio and began studies toward a Masters Degrees in Aeronautical Engineering. After graduation, DeArmond will be assigned to the Air Force Satellite Control Facility in Sunnyvale, CA.

Permanent Address: 6708 Rugby Lane
Charlotte, N.C. 28211

UNCLASSIFIED

SECURITY CLASSIFICATION OF THIS PAGE *(When Data Entered)*

REPORT DOCUMENTATION PAGE		READ INSTRUCTIONS BEFORE COMPLETING FORM
1. REPORT NUMBER AFIT/GAE/AA/82D-7	2. GOVT ACCESSION NO. AD-A124 723	3. RECIPIENT'S CATALOG NUMBER
4. TITLE *(and Subtitle)* MODAL CONTROL OF A SATELLITE IN AN UNSTABLE ORBIT		5. TYPE OF REPORT & PERIOD COVERED Masters Thesis
		6. PERFORMING ORG. REPORT NUMBER
7. AUTHOR(s) Frank M. DeArmond, Captain, USAF		8. CONTRACT OR GRANT NUMBER(s)
9. PERFORMING ORGANIZATION NAME AND ADDRESS		10. PROGRAM ELEMENT, PROJECT, TASK AREA & WORK UNIT NUMBERS
11. CONTROLLING OFFICE NAME AND ADDRESS		12. REPORT DATE December, 1982
		13. NUMBER OF PAGES
14. MONITORING AGENCY NAME & ADDRESS*(if different from Controlling Office)*		15. SECURITY CLASS. *(of this report)*
		15a. DECLASSIFICATION/DOWNGRADING SCHEDULE

16. DISTRIBUTION STATEMENT *(of this Report)*

Approved for public release; distribution unlimited

17. DISTRIBUTION STATEMENT *(of the abstract entered in Block 20, if different from Report)*

18. SUPPLEMENTARY NOTES

Approved for public release: IAW AFR 190-17.

LYNN E. WOLAVER
Dean for Research and Professional Development
Air Force Institute of Technology (AU)
Wright-Patterson AFB, OH 45433

6 JAN 83

19. KEY WORDS *(Continue on reverse side if necessary and identify by block number)*

Periodic Orbits
Lagrange Points
L3
Modal Control
Floquet Theory

20. ABSTRACT *(Continue on reverse side if necessary and identify by block number)*

See reverse side

DD FORM 1 JAN 73 1473 EDITION OF 1 NOV 65 IS OBSOLETE

UNCLASSIFIED

SECURITY CLASSIFICATION OF THIS PAGE *(When Data Entered)*

A perturbation analysis was done on a satellite in orbit about L3. A modal control scheme for linear systems was then applied to the linear and nonlinear perturbations. Rectification of the satellite orbit was achieved by Encke's Method. The effects of the moon's inclination and eccentricity on the orbit stability was investigated. The controller stabilized the linear and nonlinear perturbations, with the average control acceleration being of the same order of magnitude as that for earth-synchronous satellites.